ASSESSING THE IMPACT OF GREEN ROOFS ON THE URBAN HEAT ISLAND USING SATELLITE IMAGES: A CASE STUDY OF WASHINGTON D.C.

by

Zahra Ghaffari, M.S.

A dissertation submitted to the Graduate Council of
Texas State University in partial fulfillment
of the requirements for the degree of
Doctor of Philosophy
with a Major in Geographic Information Science
May 2021

Committee Members:

Nathan Currit, Chair

Jennifer Jensen

Russell Weaver

Jennifer Devine

FAIR USE AND AUTHOR'S PERMISSION STATEMENT

Fair Use

Duplication Permission

DEDICATION

This dissertation is dedicated to my husband, Sina, whose support, tolerance, and inspiration made it possible for me to complete this work, and to my daughter, Rona, who is a treasure in our life. And to my beloved parents who have been a source of unconditional love and encouragement.

ACKNOWLEDGEMENTS

I would like to acknowledge my advisor, Dr. Nathan Currit, for his outstanding guidance, patience, and support throughout my entire Ph.D. studies. to my committee for their continued support and encouragement: Dr. Jennifer Jensen, Dr. Rusty Weaver, and Dr. Jennifer Devine. Your feedback, comments, and suggestion were vital for writing and accomplishing this scientific research.

Also, I would like to show my gratitude towards to the amazing Geography family (department) of Texas State University, especially Dr. Rebecca Davio, Dr. Alberto Giordano, Dr. Richard Boehm, and Dr. Injeong Jo. Moreover, no words will properly express my gratitude towards our graduate staff advisor Ms. Allison Glass-Smith, her support has been priceless. Additionally, the kind and professional assistance, of Ms. Angelika Wahl, the department's administrative assistant, and Mr. Charles Robinson, the department's lab coordinator has always been easily available to me and I wish to thank them for their unconditional support and kindness.

The completion of this project could not have been accomplished without the support of my classmates, Saeide Gharechahi, Shadi Maleki, Milad Korde, Yunuen Reygadas, and Chloe Zhao. I am grateful for your support and company.

I would like to thank my parents who encouraged me through all adventures in life. I could not be where I am now without your support. You are always inspiration in my life. I love you and miss you so much. To my lovely daughter, Rona, who brought joy

and hope to my life. To my sister, Reihaneh, for her unconditional love and support. To my brother, Saleh, for his encouragements.

Finally, to my caring, loving, and supportive husband, Sina: my heartfelt thanks. I could not reach this milestone without your support.

TABLE OF CONTENTS

Page

LIST OF TABLES

Table **Page**

LIST OF FIGURES

Figure **Page**

ABSTRACT

Changing the urban environment by replacing vegetated surfaces with low albedo materials is one of the reasons for increasing temperatures in the urban environment and consequently is one of the key causes of the urban heat island effect. In urban areas, building roofs occupy a large portion of the surface area and green roofs and cool roofs are claimed to be a key approach to mitigate urban heat. Green roofs could reduce the roof top surface temperature as well as their ambient air temperature. In this study, I used satellite images to analyze the temperature of green roof buildings in Washington D.C. For the first objective of this study, I used Landsat 8 TIRS images to provide the Intra-Urban Heat Island (IUHI) pattern for Washington D.C. and performed a t-test to compare the temperatures of green and conventional roofed buildings. The result of the analysis confirms that green roofs are significantly cooler than conventional roofs. For the second objective, I used 2-way ANOVA to find the month(s) where installing green roofs had the highest impact on ambient temperature. The findings show that green roofs have cooler temperatures than conventional roofs in the warm months of the year. I then used post-treatment analysis to compare the rooftop temperature before (2009) and after green roof installation (2019). The result of this test did not confirm the hypothesis of temperature reduction due to green roof installation over the 10 year period. This may be partly attributable to the small number of green roofs in 2009. Lastly, I made two scenarios of installing green roofs on thousands of buildings citywide. The result of the third analysis shows that after hypothetically green roof installation, the impervious

surface temperature in warm months of the year is significantly cooler than before green roof installation. Therefore, this research is one of the first of this kind of study on green roofs and confirms the benefit of installing green roofs in reducing temperature over rooftops.

1. URBANIZATION, GREEN ROOFS AND THE URBAN HEAT ISLAND EFFECT

Urbanization is driven by multiple social, economic, and environmental processes, and is one of the biggest social transformations of modern time. The profound environmental impacts of urbanization vary and change over time, depending on the physical, social and economic contexts, and development trajectories. Urbanization has many positive impacts on the environment. For instance, a densely populated city tends to reduce energy-use because it requires less energy for heating and cooling. Environmentally friendly infrastructure and facilities can be easily accessible by large populations and transportation costs are reduced because people do not need to travel as far as they would otherwise. Also, higher productivity happens in urban areas because economies of scale translate to using fewer resources. In contrast, urbanization negatively impacts the environment in various ways through air pollution, water pollution, solid waste discharges, and climate change (Bai et al., 2017).

The Urban Heat Island (UHI) is a phenomenon where the ambient air temperature of an urban area is higher than its adjacent suburban and rural areas. The lack of green spaces and cool sinks, and the release of anthropogenic heat in urban areas are the causes of the UHI. Characteristics like population, building density, the relative fraction of building surfaces, the season, and the latitude all affect the strength of the UHI (Oke et al., 1991; Huang, Zhou, and Cadenasso 2011; Santamouris 2014; Razzaghmanesh, Beecham, and Salemi 2016). The UHI, in turn, affects human health, water consumption, electricity demand, and air quality and mitigating its effects is crucial for urban and

environmental sustainability. Because of population growth, infrastructure development, and urbanization, urban areas are growing rapidly across countries and understanding their dynamics and contributions to improving sustainability and addressing energy and environmental challenges is crucial (Khan & Asif, 2017). This study on the effect of green roofs on the UHI aims to improve our understanding of this important topic.

One way that urban surface temperatures can be decreased is by increasing the amount of green spaces in cities. Gill et al. (2007) showed that a 10% increase in green spaces in Manchester, UK, could gradually decrease the 4K increase in temperature that is predicted to occur over the next 80 years. In addition, Kyriakodis and Santamouris (2017) claim that urban temperatures may exceed rural temperatures by 6-7 K depending on the local characteristics and the strength of the heat sources.

In many cases urbanization tends to replace green areas with impermeable concrete surfaces, thereby reducing the space available for planting trees or other vegetation, or for implementing large-scale UHI mitigation techniques. On the other hand, increases in the number of buildings provide more rooftop surfaces which could be an excellent space to apply UHI mitigation techniques. Akbari and Rose (2008) estimated that in four big cities in the US (Chicago, IL, Houston, TX, Sacramento, CA, and Salt Lake City, UT), 20% to 25% of the city is covered by roof surfaces. One of the UHI mitigation techniques that is gaining traction is to install cool roofs and green roofs. Cool or reflective roofs aim to increase roof albedo to reduce rooftop temperatures. Green, or living, roofs, which cover the roof completely or partially with vegetation, aim to reduce rooftop temperatures by decreasing thermal gains. Besides mitigating urban heat, green roofs offer a variety of advantages like storm water retention, increased roof longevity,

decreased energy consumption, better air quality and noise reduction, and the provisioning of space for wildlife (Kalantar, Mansor, Khuzaimah, Sameen, & Pradhan, 2017; W. C. Li & Yeung, 2014; Razzaghmanesh, Beecham, & Salemi, 2016; Santamouris, 2014; Simmons, Gardiner, Windhager, & Tinsley, 2008; Yang, Yu, & Gong, 2008).

Cool roofs mitigate atmospheric heating by increasing the surface albedo and both cool and green roofs are documented as energy savers for buildings (Coutts, Daly, Beringer, & Tapper, 2013). The serious impact of large scale changes of albedo in the local ambient temperature is well documented. Campra et al. (2008) have monitored the temperature of the Almeria area in Spain for multiple years and reported that the temperature decreased by 0.3 K/decade because of massive installations of high albedo greenhouses.

Green roof design depends on many different factors, including thermal conductivity, specific heat, density, thermal absorptance, solar absorptance, height of plants, leaf area index, etc. A thick soil layer is purposely used to create thermal mass. Ashraf Muharam and ElSayed Amer (2016) showed that a 10-cm thick soil layer is sufficient to control heat penetration (Ashraf Muharam, ElSayed Amer, 2016). In another study, it was revealed that for every 10-cm increase in the thickness of the substrate layer with clay, the thermal resistance of a roof can be increased by 0.4 kW (Khan & Asif, 2017).

Many studies have used satellite images for studying the Surface Urban Heat Island (SUHI) (Cheval & Dumitrescu, 2015; Shen, Huang, Zhang, Wu, & Zeng, 2016), and many studies have used small scale *in-situ* data for modeling experiments about the

ability of green roofs to mitigate the UHI (Alexandri & Jones, 2008; Di Giuseppe & D'Orazio, 2015; Gill et al., 2007; Razzaghmanesh et al., 2016; Susca, Gaffin, Dell'osso, & Dell'Osso, 2011). Those studies that use in-situ data are generally controlled experiments that model a green roof implementation, but that do not reflect the UHI at scale. To date, there have been few efforts to use satellite images to specifically examine the city-wide effects of green roofs on mitigating the UHI. This study is one of the first to analyze the actual implementation of green roof installations as an urban cooling strategy on a citywide scale. The overarching objective of this study is to use satellite images to examine how green roof installations can affect the SUHI in a dense city like Washington D.C., a US city pioneering the installation of green roofs. It seeks to demonstrate the spatial pattern of temperatures across the city before and after green roof installations to illustrate the impact green roofed buildings have on the SUHI. I also examine monthly differences in the temperatures of green roofs compared to conventional roofs. To examine the large-scale potential of green roofs to mitigate the SUHI, I simulate total reductions in temperature by artificially applying green roofs to two scenarios of selected buildings in Washington D.C.

The remainder of this dissertation is organized as follows. Chapter 2 contains background information about the Urban Heat Island, green and cool roofs, and concludes with specific objectives and hypotheses that will be tested. The following 3 chapters correspond to 3 distinct research objectives and are treated as if they were separate papers created for peer-review. Chapter 3 is about comparing green and conventional rooftop temperatures for significant differences at a single point in time. Chapter 4 is about the effectiveness of green roofs for reducing rooftop temperatures

seasonally and annually. Chapter 5 is about the effects of hypothetical citywide installations of green roofs on the intraurban heat island. Finally, Chapter 6 summarizes the findings of the three chapters of analyses, ties them to broader questions about the Urban Heat Island, and points to some limitations and potential items for future study.

2. BACKGROUND

2.1. Urban Heat Island

Climate change, urbanization and water scarcity are the main environmental challenges in many cities around the world (Razzaghmanesh et al., 2016). According to the United Nations (2014), in 2014, 54% of the world's population was living in urban areas and it is expected that the urban population will continue to grow at such a rate that by 2050 the world will be two-thirds urban (66%). Because of population growth, infrastructure development, modernization and urbanization, cities are expanding rapidly in many countries and land previously found in a natural state is being converted to urban areas, which leads to more energy consumption and environmental problems in those urban areas (Khan & Asif, 2017; Seto, Sánchez-Rodríguez, & Fragkias, 2010). Urbanization has a considerable effect on the pattern, dynamic, and functionality of ecosystems, and therefore it is the most significant form of land-use and land-cover change (Elmqvist et al., 2013). Understanding urbanization processes and the resulting land use changes (patterns and intensities) is important for natural resources use, health, socio-demographics, and global environmental change (Elmqvist et al. 2018). Also, the geography of urbanization is changing and is predicted to have both positive and negative impacts on ecosystems and land cover. For example, households might climb up the "energy ladder" and switch from fuel wood to modern fuel resources that could reduce demand for forest resources and halt a trend of forest loss (Seto et al., 2010). Therefore, urban areas have a crucial contribution to make towards improving sustainability standards and addressing the energy and environmental challenges (Khan & Asif, 2017).

Urbanization also has a complex and multifaceted relationship with biodiversity. Often urban expansion alters the habitat configuration and connectivity of ecosystems in a way that leads to species isolation and the degradation of genetic diversity. It also can cause the loss or replacement of native species with non-native species (McKinney, 2002). Furthermore, the population dynamics and reproductivity of animals can be changed due to changes in the dynamic of UHI in cities (Bai et al., 2017).

Globally, city temperatures are continuously increasing due to climate change and the urban heat island effect, which results in a high ambient temperature, an energy consumption problem, and which threatens vulnerable populations and amplifies pollution problems (Santamouris, 2014). The increased threat of climate change has resulted in a serious focus on the UHI effect over the past few decades. As the UHI increases, the energy demand for cooling also increases (Roman, O'Brien, Alvey, & Woo, 2016; Stone & Rodgers, 2001). Heat island formation also influences air quality directly through several mechanisms. For example, the elevated atmospheric temperature can facilitate a series of chemical reactions that result in tropospheric ozone formation (Stone & Rodgers, 2001).

The "Urban Heat Island", a term coined in the English language in the 1810s (Zhao 2018) occurs when the ambient temperature of an urban area is higher compared to its adjacent suburban and rural lands because of the urban area's relatively higher density of low albedo buildings, its thermal release of anthropogenic heat, the excess storage of solar radiation by city structures, the lack of green spaces and cool sinks, the non-circulation of air in urban canyons, and the reduced ability of emitted thermal infrared radiation to escape in the atmosphere (Santamouris 2014; Di Giuseppe and D'Orazio

2015; Razzaghmanesh, Beecham, and Salemi 2016; Kalantar et al. 2017; Oke et al. 1991). The UHI also impacts the local meteorology by changing local wind patterns, forming clouds and fog, increasing humidity, changing precipitation rates, and intensifying pollutant concentration over urban areas (Mirzaei & Haghighat, 2010).

There are two types of studies in the UHI field: Atmospheric UHI (AUHI) (Howard, 1818) and Surface UHI (SUHI) (Voogt & Oke, 2003). In AUHI studies, researchers compare patterns of above-ground air temperature in urban and surrounding rural areas by collecting field data at mobile or fixed weather stations. Making field-based measurements is difficult, expensive and time consuming because of the limited number of existing stationary networks or mobile stations, and the cost of installing new measurement devices around the city. Additionally, the existing weather stations usually collect only a limited number of parameters (e.g., air temperature, velocity, turbulence, and pollution concentration). These limited and isolated stationary networks are not capable of capturing heterogeneous thermal characteristics caused by land use and land cover (LULC) (Shen et al., 2016). Moreover, using simple correlation analysis to examine relationships between measured AUHI characteristics is not accurate because there is an abundance of other parameters that could influence the AUHI formation (Mirzaei & Haghighat, 2010).

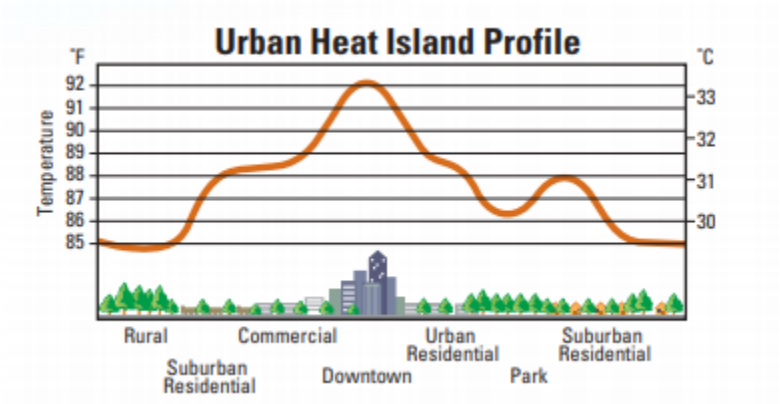

Figure 1. *An example of the urban heat island profile and cooling summertime temperatures (Strategies to reduce urban heat island. Environmental Protection Agency, 2003).*

The difference between the surface temperatures within and without an urban area is defined as SUHI and is an indirect UHI measurement method that examines the Land Surface Temperature (LST) using satellite images (Voogt & Oke, 2003). Thermal wavelengths measure the land surface temperature providing a spatially exhaustive measurement of LST which I can use to conduct UHI related research. This is in contrast to the AUHI where interpolation techniques must be applied to point-based temperature measurements to produce an exhaustive spatial representation of the AUHI. While AUHI and SUHI both measures temperature differences between urban and rural areas, they are not identical and vary non-linearly, yet neither is more accurate than the other.

Mirzaei and Haghighat (2010) summarized three categories of approaches for studying the UHI: a) Multi-scale phenomena approaches that consider "UHI formation is the consequence of several phenomena, including small scale processes like human metabolism and meso-scale interactions like atmospheric forces. Therefore, different resolutions are required to integrate all these aspects simultaneously", b) Simulation approaches which use mathematical models to solve urban climate problems like the UHI, and c) Observation approaches (Mirzaei & Haghighat, 2010). The "Observation

approaches" include three methods: 1) Field measurements, 2) Small-scale modeling, and 3) Thermal remote sensing. When using field measurements, the researcher compares the near surface temperature patterns of urban areas and rural areas as measured by pairs of fixed or mobile measurement stations (Mirzaei & Haghighat, 2010). The results are used to find the spatial distribution and intensity of the heat island inside a city. This method is expensive and time-consuming because it needs many measurement stations to be involved and only a few parameters (e.g., air temperature, velocity, turbulence, and even pollution concentration) are measured simultaneously. In the small-scale modeling approach, scientists use a small-scale physical model placed in an isolated space to simulate an urban area and this approach is mostly used to verify, calibrate, and improve the mathematical models. In the small-scale modeling approach, it is hard (and sometimes unfeasible) to ensure that all the characteristics of an actual urban situation are replicated in the small-scale physical model. It is challenging to simulate the whole study area since it is very time-consuming and expensive. In this study I use the "Thermal remote sensing" approach with Landsat 8 (band 10, wavelength of 10.60-11.19 μm) and Landsat 5 (band 6, wavelength of 10.40-12.50 μm) to calculate the surface temperature of the study area.

There has been much research using satellite images to address the SUHI using Landsat, MODIS and AVHRR imagery (Table 1). For example, Shen et al. (2016) used 26 years of high spatial resolution images for qualitative and quantitative analysis of UHI patterns, mechanisms and the evolution of Land Surface Temperature in the city of Wuhan, China. They observed that the highest temperature differences between urban and rural areas occurred in 2013 with 7.19 C differences. Cheval and Dumitrescu (2015)

used MODIS 1 km resolution images to investigate the summer surface heat island of Bucharest, Romania in terms of the city shape, intensity, extension and its links to land cover. The study claims that "the intensity calculated as the difference between the LST within the SUHI's limits and several surrounding buffers is an efficient and flexible tool for describing the average thermal state of the urban–rural transition" (pp.638-639). Azevedo, Chapman, and Muller (2016) used MODIS LST and high-resolution air temperature data from the Birmingham Urban Climate Laboratory to identify and quantify the spatial pattern of daytime and nighttime UHI in Birmingham City, UK and they found that UHI is clearly linked to land-use. They further found that the relationship between LST and air temperature was high during day and night at the neighborhood scale, but that the relationship at the city scale was weak. Weng, Rajasekar, & Hu, (2011) used ASTER thermal bands in four different seasons in different years to analyze the urban heat pattern of Indianapolis, IN. In their research they used kernel convolution modeling to characterize the UHI. They developed two new indexes (green vegetation and impervious surface) for modeling urban heat island intensity in different scales (microscale, mesoscale, regional scale). Their result shows that the UHI is highly correlated to the urban greening and impervious surface.

According to Weng (2009), AVHRR images with a 1.1-km spatial resolution were previously used to map the UHI but did not show a meaningful relationship to the ground-measured temperature. Landsat TM TIR data with 120-meter spatial resolution was then widely used for calculating LST and studying the UHI. Other examples of using Landsat TM TIR images included observations of meso-scale temperature differences, monitoring microclimate, calculating LST of building walls based on a 3-D GIS model,

and examining the relationship between LST and land-cover patterns. ETM+ images with 60-meter spatial resolution were briefly used for examining the LST-vegetation abundance relationship before the satellite malfunctioned. Later, ASTER TIR images with a 90-meter spatial resolution and that were collected both day and night, were used to study diurnal patterns of LST. As Weng (2009) mentioned, "A key issue in the application of TIR remote sensing data in urban climate studies is how to use LST measurements at the micro-scale to characterize and quantify UHIs observed at the meso-scale." For example, scientists used TIR images from AVHRR and MODIS and used different mathematical models (e.g., two-dimensional Gaussian surface superimposed, fast Fourier transformation) to quantify UHI. Also, Weng noted that applying TIR images in LST-surface energy flux relationships for characterizing landscape patterns and processes is another fundamental application of thermal imagery. The following statement by Weng (2009) is particularly relevant to this study, but also looks to a future with improved thermal imagery: "Urban climate and environmental studies will be difficult, if not impossible, without TIR sensors of global imaging capacity." Considering that the few satellites that obtain TIR images have a relatively coarse spatial resolution (mentioned in Table 1), scientists anticipate finer spatial resolution TIR images.

Thermal infrared (TIR) imagery has a variety of applications in environmental monitoring, including detecting conditions conductive to wildfire, assessing ecosystem health and drought severity, monitoring volcanic eruption activities, and exploring UHI (Agam, Kustas, Anderson, Li, & Neale, 2007). As shown in Table 1, the best freely available thermal images are from Landsat 8, 7, and 5 with the spatial resolution of 30m

after cubic convolution resampling. For this research I used images with finer spatial resolution.

Table 1: Different remote sensing sensors for studying UHI.

Sensor	**Thermal bands Spatial Resolution**	**Temporal Resolution**	**Sensor Operator**	**Research**
Thermal Infrared Sensor (TIRS)	30 m after resampling; 100 m before resampling	16 days	NASA Landsat 8	(Kikon, Singh, Singh, & Vyas, 2016)
Enhanced Thematic Mapper Plus (ETM+)	30 m after resampling; 60 m before resampling	16 days	NASA Landsat 7	(Huang, Zhou, & Cadenasso, 2010; Weng, Lu, & Schubring, 2004)
Thematic Mapper (TM)	30 m after resampling; 120 m before resampling	16 days	NASA Landsat 5	Katpatal et al. 2008; Kikon et al. 2016
MODerate resolution Imaging Spectroradiometer (MODIS)	1000 m	Twice per day	Aqua/Terra sensors, Earth Observing System (EOS) of NASA	(Azevedo et al., 2016; Cheval & Dumitrescu, 2015; Shen et al., 2016)
Advanced Very High Resolution Radiometer (AVHRR)	1.1 km	Twice per day	National Oceanic and Atmospheric Administration (NOAA)	(Shen et al., 2016)
Advanced Spaceborne Thermal Emission and Reflection Radiometer (ASTER)	90 m	16 days	NASA, METI, AIST Terra	(Weng et al., 2011)

The possible UHI causes defined by Oke (1982) are as follows: amplified short-wave radiation gain, amplified long-wave radiation gain from the sky, decreased long-wave radiation loss, anthropogenic heat sources inside urban areas, increased heat storage, less evapotranspiration and decreased turbulent heat transport.

The three-dimensional building characteristics of an urban area can impact the ambient temperature and therefore may contribute to the UHI. These characters include building height, street width, openness between buildings, and street orientation. Generally, taller buildings trap more heat energy in the urban canopy layer and reduce air

circulation, causing an increase in the surface air temperature. Also, tall buildings in narrow streets retain solar radiation through absorption by building walls, similarly raising the ambient temperature (Coseo & Larsen, 2014). Both landscape composition and configuration also influence urban thermal characteristics (Chen & Yu, 2017).

2.2. UHI Mitigation Techniques

It is essential to develop practical approaches to mitigate UHI to have a sustainable, attractive, and thermally pleasant urban environment. Also, mitigating the heat and adapting to global warming and the urban heat island effect with the smallest cost is a significant concern of governments, city managers and urban residents (Coutts et al., 2013). Two important mitigation technologies associated with roofs that help balance the thermal budget of cities are to increase thermal losses and decrease thermal gains. These technologies include increasing the albedo on the roofs and developing green spaces on the rooftops. Scientists have recorded very important climate benefits and a serious reduction of the heat island strength by applying the above mitigation technologies (Santamouris, 2014).

In the UHI phenomenon, closely spaced buildings in cities absorb solar radiation, especially when there is a lack of vegetated areas. One way the UHI can be reduced is by changing the materials used in buildings, which has positive effects for both humans and the environment (Kalantar et al., 2017). The moisture, aerodynamic, and thermal properties of cities are different in urban materials and plants, which could result in different temperatures via different process. For example, tree shading can prevent the warming of the land and air surfaces, and vegetation may affect air movement and heat exchange (Bowler, Buyung-Ali, Knight, & Pullin, 2010).

Because of urbanization, the available free ground area in an urban environment available for implementing traditional large scale mitigation techniques is very limited and the proportion of space dedicated to vegetation is minimal. On the other hand, more building structures that occupy an increasingly large proportion of a city's land surface provide roofs that are excellent spaces on which to apply mitigation techniques (Santamouris, 2014).

2.3. Green Roofs

Green roofs and cool roofs (white and/ reflective roofs) are claimed to be a key approach to mitigating the urban heat island. Green roofs could reduce rooftop surface temperatures as well as ambient air temperatures due to their thermal benefits, including the insulating effect of the soil substrate and vegetation, the shading from the plant canopy, and cooling from evapotranspiration. Among many proposed methods to reduce the UHI, green roofs seem to be an effective tool (Berardi, GhaffarianHoseini, & GhaffarianHoseini, 2014; Coutts et al., 2013; Santamouris, 2014). Cool roofs are usually white, and they can mitigate the atmospheric heating by increasing the surface albedo. Both cool and green roofs are documented as building energy savers (Coutts et al., 2013; Razzaghmanesh et al., 2016; Santamouris, 2014). Both green roofs and cool roofs are known as potential methods for reducing the UHI, but their performance depends on their design. The depth of the growing medium, plant species and water regime in green roofs are the main factors influencing green roof potential for reducing the UHI (Coutts et al., 2013). According to Dong et al. (2020), quantitative research on installed green roofs in Xiamen Island, China, effectively reduced the UHI effect in high density urban areas.

Their regression analysis revealed that rooftop LST decreases by 0.4 ˚C for every 1000 m^2 increase in green roofs.

Increasing the green spaces in big cities results in decreases in urban surface temperatures and the UHI effect. One of the methods to battle the UHI and climate change is to increase the amount of green areas on building rooftops (Razzaghmanesh et al., 2016). Gill et al. (2007) showed that covering a roof with as little as 10% green cover could reduce the surface temperature 7 - 8.2℃ in high-density residential areas and town centers respectively by 2080, compared to a 1961-1990 baseline case. Alternatively, they said that if the green covered area of roofs stayed the same, the temperature will increase by 3.3 – 3.9℃ in high-density residential areas and town centers, respectively, by 2080. In Alexandri and Jones' (2008) research about the effect of adding green roofs and green walls in 9 different cities around the world, they concluded that there is a significant reduction in the urban temperature by adding plants to buildings as green roofs and green walls. The amount of vegetation placed on the buildings is very important. The all-green buildings, with both a green roof and green walls, play a more important role in decreasing the temperature. They also have concluded that the effect of green covers on lowering urban temperatures is greater in hotter and drier climates. They claim that if green walls and roofs apply to only one block, it can create a small area of mitigated temperature. On the other hand, if it applies to the whole city, they could reduce the urban temperature to a human-friendly level and reduce the amount of energy used for cooling buildings from 32% to 100%. Likewise, Susca et al. (2011) monitored UHI in four areas in New York City and found that there is an average of 2℃ difference in temperature between the most and the least vegetated areas. They also concluded that the

replacement of black roofs with white and green roofs can reduce the overall energy consumption. Furthermore, they claim that installing green roofs instead of white roofs can result in 40-110% of energy saving.

There are many benefits to green roofs, which include, but are not limited to: enhanced aesthetic value, increased roof longevity, increase building value, stormwater runoff mitigation, potential of stormwater runoff quality improvement, air pollution reduction, noise reduction, decreased energy consumption, increased habitat for wildlife, and the ability to mitigate the urban heat island effect (Santamouris 2014; Razzaghmanesh, Beecham, and Salemi 2016; Yang, Yu, and Gong 2008; Simmons et al. 2008; Li and Yeung 2014; Kalantar et al. 2017; Coutts et al. 2013; Wolf and Lundholm 2008; Kim 2004; Khan and Asif 2017; Ahmadi et al. 2015). Details about each of the benefits of green roofs are discussed in the following paragraphs.

According to W. C. Li and Yeung (2014), green roofs date back to the gardens of Babylon and the Roman Empire when they grew trees on top of the buildings. More recently, Germany is the leader in green roof technology with more than 10% of German houses having green roofs (Köhler, 2006). Green roof buildings are also widespread in Canada and European countries like France, Switzerland, and the United Kingdom (Banting, Doshi, Li, & Missious, 2005; Herman, 2003).

Green roofs are composed of several layers. The top layer is the vegetation which is grown in a soil medium over a waterproofing membrane. Beneath the soil layer, there is a filter that prevents soil from washing away. At the bottom is a water proofing membrane layer to protect the roof. Rainwater storage is often integrated into green roofs so that collected rainwater can be reused in a dry season.

Many researchers mentioned three types of green roofs in their papers, including intensive green roofs, semi-intensive green roofs, and extensive green roofs that are differentiated by the depth of their growing medium (i.e., soil) and the types of plants grown on the roofs (e.g.: Li and Yeung 2014; Banting et al. 2005; Khan and Asif 2017; Ahmadi et al. 2015). Other researchers mentioned two different types of green roofs, namely the extensive roof with soil depths less than 150 mm and the intensive roof with soil depths greater than 150 mm. (e.g: Razzaghmanesh, Beecham, and Salemi 2016; Ashraf Muharam, ElSayed Amer 2016; Williams, Rayner, and Raynor 2010). Simmons et al. (2008) said that because green roof performance varies, they need to be designed carefully to maximize their benefits in mitigating UHI. The design of green roofs is affected by many factors like plant height, leaf area index, solar absorptance, thermal absorptance, specific heat, and thermal conductivity (Khan & Asif, 2017). Green roofs substrates need to be lightweight, chemically and physically stable, retain sufficient water and nutrients for plants, and be properly drained to avoid root saturation (Williams et al., 2010).

According to many studies, Sedum species (flowering plants with leaf succulents) are the most appropriate plant for growing in green roofs because they have shallow root systems, an ability to store water, and they experience reduced water loss due to crassulacean acid metabolism (CAM), a mechanism to reduce evapotranspiration. Aesthetically, they come in a variety of color forms (Durhman, Bradley Rowe, & Rugh, 2006; MacIvor & Lundholm, 2011; VanWoert, Rowe, Andresen, Rugh, & Xiao, 2005; Williams et al., 2010). Banting et al. (2005) listed various types of plants for three different green roof types (Extensive, Semi-Intensive, and Intensive green roofs) based

on their growing medium depth. The plants for extensive green roofs in four different medium depth includes Moss-sedum, Sedum-Moss-herbaceous plants, Sedum-herbaceous-grass plants, and Grass-herbaceous plants. They listed four different medium depths which could hold Grass-herbaceous plants, Wild shrubs-coppices, coppices and shrubs, and coppices. They classified medium depth for Intensive green roofs into seven classes including depths appropriate for lawn grass, low-lying shrubs and coppices, medium height shrubs and coppices, tall shrubs and coppices, large bushes and small trees, and large trees. The plants for the extensive green roofs, the most common type of green roof, have the following characteristics: a) an ability to establish themselves quickly and reproduce efficiently, b) a short height that is cushion or mat-forming, c) a shallow root system, and d) an ability to store water in succulent leaves (MacIvor & Lundholm, 2011; Snodgrass & Snodgrass, 2006). Because there is a negative relationship between drought resistance and transpiration, drought resistance plant are most often used for optimal green roof functioning (Wolf & Lundholm, 2008).

Coutts et al. (2013) used sedum as the vegetation in their study of green roof beds which suggested that green roofs can perform efficiently in providing microclimate benefits when in good irrigation condition. If the green roof is a bed with a mixture of actively transpiring plants that are irrigated regularly, they can provide as much benefits as white roofs. Even though sedum are the most commonly used plant species in green roofs due to their drought tolerance, ability to reduce storm water runoff, and their shallow roots, they are not ideal plants for cooling ambient temperatures. For the cooling purposes of the green roofs, the selected plants should have a high transpiration rate to be able to enhance the evaporative cooling effect. They also suggested covering the soil in

green roofs with a thin layer of white gravel or stone to increase the albedo (Coutts et al., 2013). The texture of leaves is also important for their cooling ability (Blanusa et al., 2013; Coutts et al., 2013; W. C. Li & Yeung, 2014; Wolf & Lundholm, 2008). Blanusa et al. (2013) conducted a study about the cooling potential of different plants. They examined the leaf morphology, the effect of leaf surface temperature on its immediate above canopy temperature, and the effect of plant type on the below canopy temperature. Their results showed that *Stachys* perform better in all three aspects compared to other two species in their experiment (*Bergenia cordifolia,* and *Hedera Hibernica*).

Another benefit of installing green roofs in managing runoff is their ability to delay peak runoff from impermeable surface areas, which is a problem that increased the frequency, volume, and peak flow from storm water runoff. Reducing storm water runoff is often considered the biggest benefit of green roofs since a large proportion of urban impermeable surfaces are covered by roofs. (Carter & Fowler, 2008; Elliott et al., 2016; Getter, Rowe, & Andresen, 2007; Y. Li & Babcock, 2014; Oberndorfer et al., 2007; Walsh et al., 2005). With green roofs, peak runoff can be delayed by up to 10 minutes in 57% of cases and the runoff rate decreases from 4.3 mm/h to the average of 2.4 mm/h (Simmons et al., 2008). The organic matter content increases from 2% to 4% over five years after green roof installation and pore space increase from 41% to 82%, which increases a green roof's capacity for holding water from 17% to 67% (Getter et al., 2007). Increasing the depth of the growing medium reduces total and peak runoff by increasing the capacity for water retention. Other factors that affect water retention and the overall capacity for water storage include the type of the green roof, the type of growing medium, the drainage layer, the runoff dynamics, the intensity of rain event, the types of

plants, the areal coverage of green roofing materials, the seasonal variations, the slope, and the age of the green roof (Banting et al., 2005; Bengtsson, Grahn, & Olsson, 2004; Getter et al., 2007). The substrate plays a more important role than vegetation for water retention. For example, Banting et al. (2005) indicated that extensive green roofs can store 40% to 60% of total rainfall, while the ability for water storage in semi-intensive and intensive green roofs depends on the areal coverage of the green roof. Water retention varies from 100% for precipitation events less than 10 mm, to 26% to 88% for precipitation events of 12 mm, depending on the green roofing materials. Based on VanWoert et al. (2005), the substrate alone can store 50.4% of the rainfall while a vegetated roof increases it to 60.6%. During warm seasons, the retention ability increases due to higher evapotranspiration which leads to faster water storage regeneration (MacIvor & Lundholm, 2011).

Water stored in plants should ideally be transpired or evaporated from the soil before the next rain fall event to regenerate the green roof water retention capacity (Stovin, Poë, & Berretta, 2013). Therefore, an appropriate plant for a green roof should be able to tolerate frequent drought periods and absorb and retain rainwater. It is for these reasons that succulents in the genus *sedum* are common plant species used in green roofs as a conservative water strategy (VanWoert et al., 2005; Villarreal & Bengtsson, 2005). However, Farrell et al. (2013) said that succulents may result in a green roof's reduced ability to loose water may negatively impact ability to regenerate the soil water capacity prior to the next precipitation event. Therefore, appropriate plants should be able to quickly lose water by transpiration after each rainfall event and also have high drought tolerance by limiting their transpiration to be able to survive dry substrates between

rainfall events (Farrell et al., 2013; Wolf & Lundholm, 2008). Zhang et al. (2018b) concluded that monocultures have a higher capacity to retain rainwater than polycultures. Polycultures had higher biomass and productivity but not higher water retention. Zhang et al. (2018b) suggested that plant root traits should be considered in addition to plant diversity and water use strategies. Williams, Rayner, and Raynor (2010) said that native species are more suitable for planting on green roofs because they are aesthetically pleasing, they are already adapted to the prevailing climate, they can benefit biodiversity conservation, and they are known, culturally significant plants.

Since green roofs reduce runoff, they also decrease pollutant loads (nitrogen, lead, zinc) (Gregoire and Clausen, 2011). The effect of acid rain is reduced by green roofs due to increases in the pH of runoff water. Similarly, air pollution is reduced by green roofs because they absorb airborne pollutants (W. C. Li & Yeung, 2014). Green roofs can reduce carbon, dust, nitrates, and other particulates (Yang et al., 2008). Yang, Yu, and Gong (2008) studied the green roof potential for removing air pollutants in Chicago using a dry deposition model. Their research results showed that the 19.8 ha of green roofs removed a total of 1675 Kg of air pollutants in one year and suggested that the total air pollutants removed could increase to 2046.89 metric tons if all rooftops were covered by intensive green roofs.

Energy savings due to the insulation provided by a green roof is another benefit of installing a green roof. The energy saving performance of green roofs depends on climatic conditions, building energy function, insulation of the building, type of green roof and the thickness of the growing medium, vegetation density and leaf area index (Ahmadi et al. 2015). Susca et al. (2011) claim that green roofs are capable of reducing

the amount of energy used for cooling and heating and are capable of mitigating peak energy usage. They said that installing green roofs can save energy from approximately 40% - 110% compared to white (cool) roofs. Research shows that residential energy consumption increases with urban temperature and Akbari (1992) claims that when the temperature increases 0.5℃ in summer in US cities, the peak electricity load for cooling increases by 1.5 – 2%. Green roofs are known as a passive strategy to reduce consumed energy in different climates by working as insulation. Green roofs reduce greenhouse gases and save energy while enhancing the aesthetic qualities and architectural presentation of buildings (Khan & Asif, 2017). The energy saving performance of green roofs depends on climatic conditions, building function, insulation of the building envelope and the type of green roof. While green roofs provide shade, insulation, and evapotranspiration against solar radiation, they also reduce the indoor air temperature in summer. During winter, green roofs act as wind shields and reduce heating loads, but the temperature regulating effect during winter is less than in summer (Khan & Asif, 2017). The impact of green roofs on energy savings is significantly higher in non-insulated buildings compared to insulated buildings and the reduction of the annual energy load may vary from 1% to 40% in extreme cases for various types of buildings, green roof characteristics and climate zones (Santamouris, 2014). Good green roof design depends on many different factors and a thick soil layer is purposely designed to create thermal mass. A research study shows that to control heat penetration, a 10-cm thick soil layer is sufficient (Ashraf Muharam, ElSayed Amer, 2016). In another study (N. H. Wong et al., 2003), it is revealed that for every 10-cm increase in the thickness of the substrate layer with clay, the thermal resistance of the roof can be increased by 0.4 kW (Khan & Asif

2017). The hydrological design of the green roofs is also important in the rooftop energy balance and therefore in the rooftop microclimate (Metselaar, 2012).

Biodiversity is another benefit of green roofs located in urban areas. Studies showed that a wide range of plant, bird and invertebrate species have been seen on green rooftops. Kim (2004) said that it is very important to install well-created green roofs and link fragmented habitats to support animals and plants with the goal of conserving urban biodiversity.

One of the factors that should be considered in installing green roofs is the cost of installing and maintaining them. The cost of green roofs is more than conventional and cool roofs and depends on the type of green roof (i.e., the depth of the medium, the vegetation types, and the drainage system type) as well as maintenance costs. According to the U.S. Environmental Protection Agency (2008), the cost of green roofs can vary from 100 $/m^2 to 250 $/m^2 in United States. They mention that the installation price may decline when market demand and contractor experience increase.

In recent years remote sensing satellites have been used widely to provide land surface temperature (LST) continuously. Although the land surface temperature is not equal to the air temperature in the urban canopy layer, studies have confirmed that LST is highly correlated with near ground air temperature and is reliable to examine the relationship between UHI and urban surface parameters (Dong et al., 2020; Voogt & Oke, 2003). As mentioned previously, there has been much research about the UHI and how it affects urban environments and humans (Azevedo et al., 2016; Cheval & Dumitrescu, 2015; Peng, Xie, Liu, & Ma, 2016; Shen et al., 2016). Numerous studies have revealed that green roofs have the potential to cool urban environments. However,

these studies have either been conducted on a small scale, observing individual instances of cooling method applications (Ashraf Muharam, ElSayed Amer, 2016; Blanusa et al., 2013; Coutts et al., 2013; Köhler, 2006; Simmons et al., 2008; Susca et al., 2011), or they have been attempts to mathematically model what would happen if such methods were adopted on a city or regional scale (Alexandri & Jones, 2008; Asadi, Arefi, & Fathipoor, 2020; Khan & Asif, 2017; J. K. W. Wong & Lau, 2013). While green roof is mentioned to be an effective way to reduce the rooftop temperature and consequently reduce the UH, few empirical studies have focused on the cooling effect of green roof at urban scales (e.g. Dong et al., 2020). In this study I want to quantify the cooling effect of green roofs in Washington D.C., where more than one million square meters of installed green roof were reported in 2017.This study is one of the first to present data regarding the installation of actual green roofs as an urban cooling strategy on a city scale. Since the study area is limited to the city boundary of Washington D.C., I use the term intra-urban heat island (IUHI) after Yokobori & Ohta, (2009) to describe temperature differences between dense built-up areas and natural areas within the city. In this study I use satellite images to examine how green roof installations in Washington D.C., a dense city that is one of the pioneers in the US for installing green roofs, can affect the UHI. The objective of this study is to quantify the cooling effect based on real green roof projects in high-density urban areas at the city scale to address the following research questions:

1. Do green roofed buildings have discernibly lower temperatures than conventional roofs? Do green roofs mitigate the IUHI in a significant way across a city?
2. Has the installation of green roofs significantly decreased the temperature of buildings in Washington D.C. over time? Does the IUHI vary by season? Do

green roofed buildings experience smaller fluctuations in surface temperature in different seasons?

3. To what extent would the IUHI be reduced if a specific portion of buildings in D.C. installed green roofs? What is the large-scale potential of green roofed buildings for mitigating the IUHI across an entire city?

The objectives of this research derive from the above questions and are to: a) examine the differences between green roof building temperatures compared to regular roofed buildings in 2019, b) compare rooftop temperatures before and after installation of green roofs (2009 and 2019, respectively) and explore temporal trends in the magnitude of those temperatures, and c) simulate the change in the IUHI if exhibited changes in temperature were extended to multiple selections of buildings across Washington D.C. To fulfill these objectives, the following analytical steps will be completed:

Pre-processing:

1- Detect green roofed buildings from official city reports.
2- Obtain satellite images from Landsat 5 and 8.
3- Convert image digital numbers of thermal bands to temperatures in degrees centigrade.

Objective 1:

1- Determine the distribution of surface temperatures in Washington D.C. by using processed satellite images to create a heat island map.
2- Perform a conventional t-test to compare the temperatures of green and conventional roofed buildings.

Null hypothesis: There is no temperature difference between green roofs and conventional roofs.

Alternative hypothesis: The surface temperature for green roofs is lower than for conventional roofs.

Objective 2:

3- Determine the month(s) that green roofs have their highest impact on their ambient temperatures by using 2-way ANOVA to consider the following hypotheses:

Null hypothesis: There is no difference in green roof temperatures in different months.

Alternative hypothesis: There is a difference in green roof temperatures in different months.

4- Compare rooftop temperatures before and after green roof installation by using post-treatment analysis to demonstrate if the changing pattern of the urban temperature is a result of green roof installations.

Null hypothesis: There is no difference in rooftop temperatures after green roof installations.

Alternative hypothesis: Rooftop temperatures are cooler than they were after green roof installation.

Objective 3:

5- Create two green roof models of Washington D.C. by applying green roof temperatures to selected building rooftops to examine if such hypothetical green

roof installations would reduce the IUHI. The two green roof model scenarios are:

a) Installation of green roofs on 10% of buildings in each Washington D.C. ward by using specific criteria for selecting buildings.

b) Installation of green roofs on building rooftops in accordance with the City of Toronto green roof bylaw policy.

3. A COMPARISON OF GREEN AND CONVENTIONAL ROOF TEMPERATURES

3.1. Introduction

Urban areas contribute to climate change, and inversely, climate change is a major threat for urban areas worldwide (Seto, Sánchez-Rodríguez, and Fragkias 2010). An enhanced Urban Heat Island (UHI) is one of the main consequences of climate change. In this phenomenon the ambient temperature of the urban area is higher compared to its adjacent suburban and rural areas due to the thermal release of anthropogenic heat and the lack of green spaces and cool sinks. The strength of the UHI varies with population, building density, the relative fraction of building surfaces, the season, and the latitude. In addition, the excess storage of solar radiation by urban structures such as tall buildings, reduces air circulation in urban canyons as well as the ability of emitted infrared radiation to escape into the atmosphere, which all cause an urban heat island (Oke et al., 1991; Huang, Zhou, and Cadenasso 2011; Santamouris 2014; Razzaghmanesh, Beecham, and Salemi 2016).

The Surface Urban Heat Island (SUHI) is defined as the difference between the surface temperatures within and without an urban area and is an indirect UHI measurement method that examines the Land Surface Temperature (LST) using satellite images (Voogt & Oke, 2003). Thermal waveengths measure the land surface temperature providing a spatially exhaustive measurement of LST which I used to conduct this UHI research.

Because of urbanization and the replacement of green areas by impermeable surfaces, the available free ground area in an urban environment on which to implement large scale UHI mitigation techniques is very limited and the proportion of land dedicated to plants and trees is often less than before urbanization. At the same time, because of increases in building developments, roofs provide an excellent space to apply UHI mitigation techniques (Santamouris 2014). Akbari, Menon, & Rosenfeld (2009) estimated that in four cities in the US (Chicago, IL; Houston, TX; Sacramento, CA; and Salt Lake City, UT), 20% to 25% of the city is covered by roof surfaces.

Implementing practical approaches to mitigate urban heat at low cost to adapt to global warming, extreme heat events, and urban heat effects is a concern for governments, city managers, and urban residents (Coutts et al. 2013). Green roof installation, which covers the roof completely or partially with vegetation, is a roof related UHI mitigation technique. The vegetation of green roofs is grown in a soil medium over a waterproofing membrane, to protect the roof, and beneath is a filter to prevents soil from washing away (Santamouris, 2014).

Scientists have recorded very important climate benefits and a large reduction of the urban heat island intensity by applying the above mitigation technique in controlled experiments (Santamouris 2014). Green roofs reduce the rooftop surface temperature as well as ambient air temperature due to the roof's thermal benefits, including the insulating effect of the soil substrate and vegetation, the shading from the plant canopy and transpirational cooling.

Washington D.C. is ranked first in the nation for green roof installations and has registered more than 1 million square feet of green roofs. The Department of Energy and

Environment in Washington D.C. is offering funds and rebates for installing green roofs to encourage voluntary green roof installation around the District. Since I examine the temperature via thermal images only within the city border of D.C., I use the term of intra-urban heat island (IUHI) to describe the temperature differences within the city, as did Yokobori and Ohta (2009) in Tokyo, Japan.

There are many studies that use satellite images for studying the SUHI (Shen et al. 2016; Cheval and Dumitrescu 2015), and many studies that use small scale in-situ data for modeling the ability of green roofs to mitigate the UHI (Alexandri and Jones 2008; Di Giuseppe and D'Orazio 2015; Gill et al. 2007; Susca et al. 2011; Razzaghmanesh, Beecham, and Salemi 2016). Those studies that use in-situ data are generally controlled experiments that model a green roof implementation, but that do not reflect the UHI at scale. To date, minimal research has been conducted to use satellite images to specifically examine the city-wide effects of green roofs on mitigating the UHI. This study is one of the first to analyze the actual implementation of green roof installations as an urban cooling strategy on a city-wide scale. The overarching objective of this study is to use satellite images to examine how green roof installations affect the UHI in a dense city like Washington D.C., a US city pioneering the installation of green roofs. I demonstrate the spatial pattern of temperature across the city by using processed satellite images to create a heat island map. The null hypothesis is that the temperatures of green and conventional roofs do not have significant differences. To examine this hypothesis, I compare green rooftop temperatures with conventional rooftop temperatures by performing a t-test to find out if green roofed buildings have discernibly lower temperatures than conventional roofs or not.

3.2. Data and Methodology

3.2.1. Study Area

Washington D.C., the capital of the United States of America, is surrounded by the States of Maryland and Virginia and has a total surface area of 176.99979 km^2 and the population of 681,170 based on the 2016 census. It is a compact city with more than 161,000 buildings. Based on the Köppen–Geiger climate classification, Washington D.C. has a "Humid Subtropical" climate. According to the National Weather Service (Washington D.C. Temperature, 2020) the 2019 average temperatures for winter, spring, summer, and autumn were: 4.2, 15.6, 26.4, 16.7 C respectively, the annual temperature is 15.9 C, and the annual precipitation in 2019 was 107.5 cm (Washington D.C. Precipitation, 2020).

3.2.2. Data

The data required to meet the objectives of this research include building footprints and building attributes inherent in and derived from other data, including the roof type, building height, proximity to green spaces, building density and rooftop temperature. Geospatial data for the Washington DC city boundary, building footprints, parks and green space locations, and lidar data were gathered from the Washington DC Open Data Portal (April 2019). The building footprints and parks datasets was originally captured in 2015 and updated in 2017 and 2019 as maintained by the Washington DC Open Data Portal. Building roof types were identified in the Best Management Practice (BMP) dataset also available on the Washington DC Open Data Portal. This dataset was collected and maintained over a 19-year (from 2001 to 2020) period for documenting structural controls used to manage stormwater runoff. The lidar data was collected on April 5, 2018 during a

leaf-on period. The downloaded lidar data had been preprocessed to a normalized digital surface model (nDSM) that represents DC's surface and its height above the ground surface.

Rooftop temperatures were derived from Landsat 8 satellite imagery consisting of nine spectral bands from the Operational Land Imager (OLI), and two thermal bands from the Thermal Infrared Radiometer (TIRS). Bands 10 (10.60 – 11.19 μm) and 11 (11.50 - 12.51 μm) measure land surface temperature at 100-meter resolution, but the data is resampled using cubic convolution and the product is delivered at a 30-meter resolution. All Landsat 8 imagery was obtained from the USGS Earth Explorer (https://earthexplorer.usgs.gov/). PlanetScope™ (https://www.planet.com/explorer/) images were obtained for verifying the presence of green roof buildings. PlanetScope imagery has blue, green, red, and near-infrared wavelength bands with a spatial resolution of approximately 4 meters. Since the month of May is one of the greenest months in Washington D.C. area, I obtained PlanetScope images for May 2019 and calculated NDVI from them.

3.2.3. Study UHI Techniques

Mirzaei and Haghighat (2010) summarized three approaches to study the UHI: a) the multi-scale phenomena approach, which describes UHI formation as the consequence of several multi-scale phenomena including human metabolism at the local scale, and atmospheric forces at the meso-scale; b) simulation approaches that use mathematical models and computational techniques to model the UHI; and c) observation approaches. Within the “observation approaches” there are three different techniques: 1) field

measurement, 2) small-scale modeling, and 3) thermal remote sensing. In the field measurement approach the researcher compares the near surface temperature patterns of urban areas and rural areas using measured pairs of fixed or mobile measurement stations. The results are used to find the spatial distribution and intensity of the heat island inside a city. This method is expensive and time-consuming because it needs many measurement stations to be involved and only a few parameters (e.g., air temperature, velocity, turbulence, and even pollution concentration) can be measured simultaneously. In the small-scale modeling approach, scientists use a small-scale physical model placed in an isolated space to simulate an urban area and this approach is mostly used to verify, calibrate, and improve the mathematical models. In the small-scale modeling approach, it is hard (and sometimes unfeasible) to ensure that all the characteristics of the actual urban situations are replicated in the small-scale physical model. It is challenging to simulate the whole study area since it is very time-consuming and expensive. In this study, therefore, I used the "thermal remote sensing" method using Landsat 8 thermal images.

3.2.4. Building Attribution

The Washington DC city boundary file was used to confine our image analysis to the Washington DC city limits. The building footprints file was used to identify the spatial location of building rooftops. Building attributes were derived from other data, including the Best Management Practice (BMP) dataset to identify green roofed buildings. The BMP dataset contained attributes for 161,519 buildings that corresponded to those found in the building footprint file and included building heights and roof types. These data were used to calculate per building average surface temperatures from remotely sensed imagery. I also

calculated building density and building proximity to green spaces within the city based on the BMP and building footprints datasets.

The building footprint data was combined with the building attribute data to find the best match for each green roof building among conventional roof buildings. Three-hundred and eighty buildings were identified as “extensive green roof”, “intensive green roof”, or “green roof” by the BMP, but a manual check of these roofs using PlanetScope imagery indicated that several buildings were not actually covered with vegetation. It could be that the BMP data was not updated, or that the green roof portion of the rooftop was so small that it did not appear vegetated. Moreover, there are several parking lots and ground level buildings categorized by the BMP as green roofs that I did not use because they do not have building rooftops. I therefore decided to use the Normalized Difference Vegetation Index (NDVI) to identify existing green roof buildings from among the 380 identified by the BMP. NDVI is the ratio of the difference in near-infrared and red bands to the sum of near-infrared and red bands where larger NDVI values correspond to vegetation. I calculated the mean NDVI value for each building roof top and then, following the methodology of Park & Cho (2016), identified those buildings with a mean NDVI greater than 0.25 as having green roofs. This threshold yielded 156 buildings from among the previous 380 buildings that were identified by the BMP as having green roofs.

Since building height can impact the ambient temperature and therefore may contribute to the UHI (Coseo & Larsen, 2014), I used a nDSM (normalized Digital Surface Model) to obtain building heights. The nDSM is an elevation dataset representing both the ground surface and the height of features above the ground surface

(opendata.DC.gov). I used Zonal Statistics to calculate the average height of each building from the nDSM point cloud.

Increases in the amount of green areas could decrease the urban surface temperature and the UHI effect. It follows, therefore, that nearby green areas could affect the temperature of buildings and so I calculated the distance of each building from its nearest green area. For this purpose, I downloaded "Parks and recreation areas" and "National Parks" shapefiles from DC.gov website. After merging them, I used the NNJoin package in QGIS to calculate the distance of nearest green space to each building.

Because the density of urban buildings also contributes to the strength of the UHI (Razzaghmanesh et al., 2016), I calculated a building density metric for each building. The average building footprint in Washington, DC is approximately 160 m^2, or approximately 13 m x 13 m, and a 170 m buffer was selected as a reasonable distance around each building to encapsulate neighboring buildings. The building density metric I created was the ratio of building area to total ground area within a buffer around each building. The mean and median building density values for Washington DC are 0.76 and 0.33 respectively, and the minimum and maximum values are 0.14 and 50.86. A low ratio value means that lower building density exist surrounding the buildings and a high ratio value means that the density of existing buildings around that building is high. So the mean and median values taken together mean that the average building area-to-ground area ratio is large, relative to the total area of surrounding buildings. The median value means that 76% of the buffer area is covered by buildings—that most of the area is covered by buildings. Thus, high building density.

In brief, I gathered and processed building height, building area, distance to parks and open spaces, and surrounding building density data to create a geospatial dataset for my research. Once all this data was prepared, I processed thermal data as outlined below and analyzed them to answer my research questions.

3.2.5. Land Surface Temperature (LST) Retrieval

Raw Landsat 8 thermal imagery needs to be converted to surface temperatures through the following processing steps. First, the digital number (DN) of the thermal infrared band is converted to spectral radiance by using the following equation:

$$L_\lambda = ML*Qcal + AL, \quad (1)$$

where, L_λ= spectral radiance (W/(m2 * sr * μm)), ML= radiance multiplicative scaling factor for the band (RADIANCE_MULT_BAND_n from the metadata), AL= radiance additive scaling factor for the band (RADIANCE_ADD_BAND_n from the metadata), Qcal= level 1 DN.

L_λ is then converted to surface-leaving radiance (L_T) through an atmospheric correction process using:

$$L_T = (L_\lambda - L_\mu - \tau(1-\varepsilon) L_d) / \tau\varepsilon, \quad (2)$$

where, L_μ and L_d are upwelling and downwelling radiance, respectively, and τ is the atmospheric transmission. These factors were calculated using a web-based atmospheric correction tool (available at: https://atmcorr.gsfc.nasa.gov/) developed by Barsi et al. (2005). The term ε is the emissivity which is defined as the emittance ratio of an object in relation to a black body at the same temperature, which is calculated as (USGS and NASA 2015, pp.265):

ε = radiance emittance from an object / radiance emittance from a black body at the same temperature.

One of the challenges with calculating surface temperature using thermal images is the varying degrees of correlation between satellite-measured thermal radiance and the actual surface temperature that is attributable to varying emissivities of different surface objects (Artis and Carnahan 1982). That is, knowing the emissivity of an object is necessary in order to correlate its temperature with a measured value of radiated thermal energy. Of the many different methods to calculate emissivity, an easy-to-apply procedure is to use the Normalized Difference Vegetation Index (NDVI) Threshold Method. The TOA reflectance was calculated by converting the Landsat 8 DNs for red and near-infrared bands using below equation:

$$\rho_{\lambda'} = M\rho\, Q_{cal} + A\rho, \quad (3)$$

where, $\rho_{\lambda'}$ = TOA planetary reflectance, without correction for solar angle.
$M\rho$ = band-specific multiplicative rescaling factor from the metadata (REFLECTANCE_MULT_BAND_x, where x is the band number), $A\rho$ = band-specific additive rescaling factor from the metadata (REFLECTANCE_ADD_BAND_x, where x is the band number) and Q_{cal} = quantized and calibrated standard product pixel values (DN)
The NDVI Threshold method obtains the emissivity values by using below equation:

$$\varepsilon = \varepsilon_v F_v + \varepsilon_u (1 - F_v) + d\varepsilon, \quad (4)$$

where, ε_v is the emissivity of vegetation and ε_u is the emissivity of urban surface. According to previous studies (Artis and Carnahan 1982; Peng et al. 2016; Nichol 1998; Nichol 1994; J. Li et al. 2011; Sobrino, Jiménez-Muñoz, and Paolini 2004; Zhao 2018), the emissivity of vegetation is typically 0.99, and the emissivity of urban surfaces is 0.92. In

Equation 5, F_v refers to the vegetation fraction which can be calculated by using below equation:

$$F_v = [(NDVI - NDVI_{min}) / (NDVI_{max} - NDVI_{min})]^2, \quad (5)$$

In Equation 5, $NDVI_{max}$ is equal to 0.5 and $NDVI_{min}$ is equal to 0.2 (Peng et al. 2016; Zhao 2018).

Also, in Equation 4, the term $d\varepsilon$ refers to the effect of the geometrical distribution of the natural surfaces and also the internal reflections. For plain surfaces, this term is negligible, but for heterogeneous and rough surfaces, like for forests, the value of $d\varepsilon$ can reach 2% (Sobrino, Jiménez-Muñoz, and Paolini 2004). A good approximation for this term can be given by Equation 6:

$$d\varepsilon = (1 - \varepsilon_u) (1 - F_v) F\varepsilon_v, \quad (6)$$

where, F is geometrical factor, with a mean value is 0.55, assuming different geographical distributions (Sobrino, Jiménez-Muñoz, and Paolini 2004; Zhao 2018).

Taking into account Equations 4 and 6, the final equation for emissivity is given by Equation 7 (Peng et al. 2016; Sobrino, Jiménez-Muñoz, and Paolini 2004):

$$\varepsilon = 0.02644 F_v + 0.96356 \quad (7)$$

Once L_T is calculated according to equations 2 through 7, the TOA brightness temperature is calculated using the following conversion equation:

$$T_B = K_2 / \ln (K_1 / L_T + 1), \quad (8)$$

where, T_B is the TOA brightness temperature (K), L_T is TOA spectral radiance (Watts/(m^2 * srad *µm)), K_1 and K_2 are band specific thermal conversion constants obtained from the metadata (USGS and NASA 2015, pp.55).

Now that I have the temperature at the sensor and the emissivity, I can calculate the surface temperature by using the below equation:

$$T = T_B / (1 + ((\lambda T_B) / \alpha) \ln \varepsilon), \quad (9)$$

where, T_B is the brightness temperature (here it is the temperature at the Landsat 8 sensor), λ is the wavelength of emitted radiance (m), α is a constant ($hc/K = 1.438 \times 10^{-2}$ mK), and ε is emissivity where I calculated by using equation 7 (Artis and Carnahan 1982).

I applied the above equations to a Landsat-image from July 2019 to produce surface temperatures in degrees centigrade and then extracted the minimum, maximum, and mean temperatures for each building using a zonal statistics tool. This final thermal pre-processing was combined with the previously created geospatial building attributes to create a complete set of building attributes that allowed us to proceed to the next step of comparing the temperatures of green and conventional rooftops.

3.2.6. Comparing Rooftop Temperatures for Green and Conventional Roofs

Having developed a dataset that includes building rooftop temperatures and many building attributes that are hypothesized to influence those temperatures, I proceeded to analyze the existence of differences between green roofed and conventional roofed buildings. I used the collected building attribute data in conjunction with propensity score matching to select samples of similar conventional roof buildings to compare to the green roof buildings. For this purpose, I used the MatchIt package in R to find the best match between green roof and conventional roof buildings. Using the MatchIt package helped me to find the conventional roof buildings that best matched the characteristics of green roof buildings. I tried to find the match of 156 green roofs among 161,363 conventional roof

buildings, but the result was not satisfying since it was a great range of building criteria. To optimize the search, I put threshold for each criterion for conventional roof buildings and these thresholds were the same as the min and max value in green roof buildings criteria.

After finding the best match among conventional roof with regular roofs, I used a two-sample t-test for independent observations to compare the mean roof temperature of the selected green roof buildings to the mean temperature of the selected conventional roof buildings to see if there is a significant difference between them or not. A two-sample t-test for independent observations uses the following equations (10 and 11):

$$T = (\mu_G - \mu_R) / SE_{(\mu G - \mu R)}, \quad (10)$$

$$SE_{(\mu G - \mu R)} = \sqrt{((S_G^2) / n_G + (S_R^2) / n_R)}, \quad (11)$$

$$S_G^2 = (\sum_{(i=1)}^{(n_G)} (G_i - \mu_G)^2)/(n_G - 1),\ S_R^2 = (\sum_{(i=1)}^{(nR)} (R_i - \mu_R)^2)/(n_R - 1), \quad (12)$$

$$df = [(S_G^2)/n_G + (S_R^2)/n_r]^2 / [(((S_G^2)/n_G)^2 / (n_G - 1) + ((S_R^2)/n_R)^2 / (n_R - 1))] \quad (13)$$

where, SE: standard error of the difference in the Aspin-Welch unequal-variance T-test, S_G^2: Green Roof Building Temperature Variance, S_R^2: Regular Roof Sample Building Temperature Variance, μ_G: Mean of temperature of Green roof data set, μ_R: Mean of temperature of Regular roof data set,

n_G: Number of items in Green roof data set, which is 156 in this study, n_R: Number of items in Regular roof data set, which is 156 in this study, df: degree of freedom using Satterthwaite's approximation.

I then calculate the t-test and p-value by considering 95% confidence level to present statistical significance. The result of the test in presented in the next section.

3.3. Results

I used a July 27th, 2019 Landsat satellite image to calculate the temperature in degrees centigrade using band 10. The heat map of Washington D.C. (Figure 2) shows that the temperature ranges from 22.9 to 50.9 ˚C. The coolest areas (shown in shades of green) are "Rock Creek Park and Pinery Branch Parkway" with an area of 2.741 mi^2 located on the northwest part of the city. The warmest part of the city (shown in shades of orange-red), are mostly located on northeast of the city which is defined as a Production, Distribution, and Repair (PDR) zone that was established by the 2016 Zoning Regulations of the District of Columbia. These zones allow heavy commercial and light manufacturing activities that require some heavy machinery use. Areas dominated by green colors are either natural areas, low-density, wooded residential neighborhoods or parks and recreational areas. Heavily built-up areas like the PDR and downtown zones are the warmest parts of the city where there are fewer green areas. The satellite imagery that I used had a 30-meter spatial resolution and is not the optimum resolution to look at rooftops, but since these images are the only freely accessible images that provide thermal data, they were my best option. The thermal image, however, provided a good resource to show the heat map of the city.

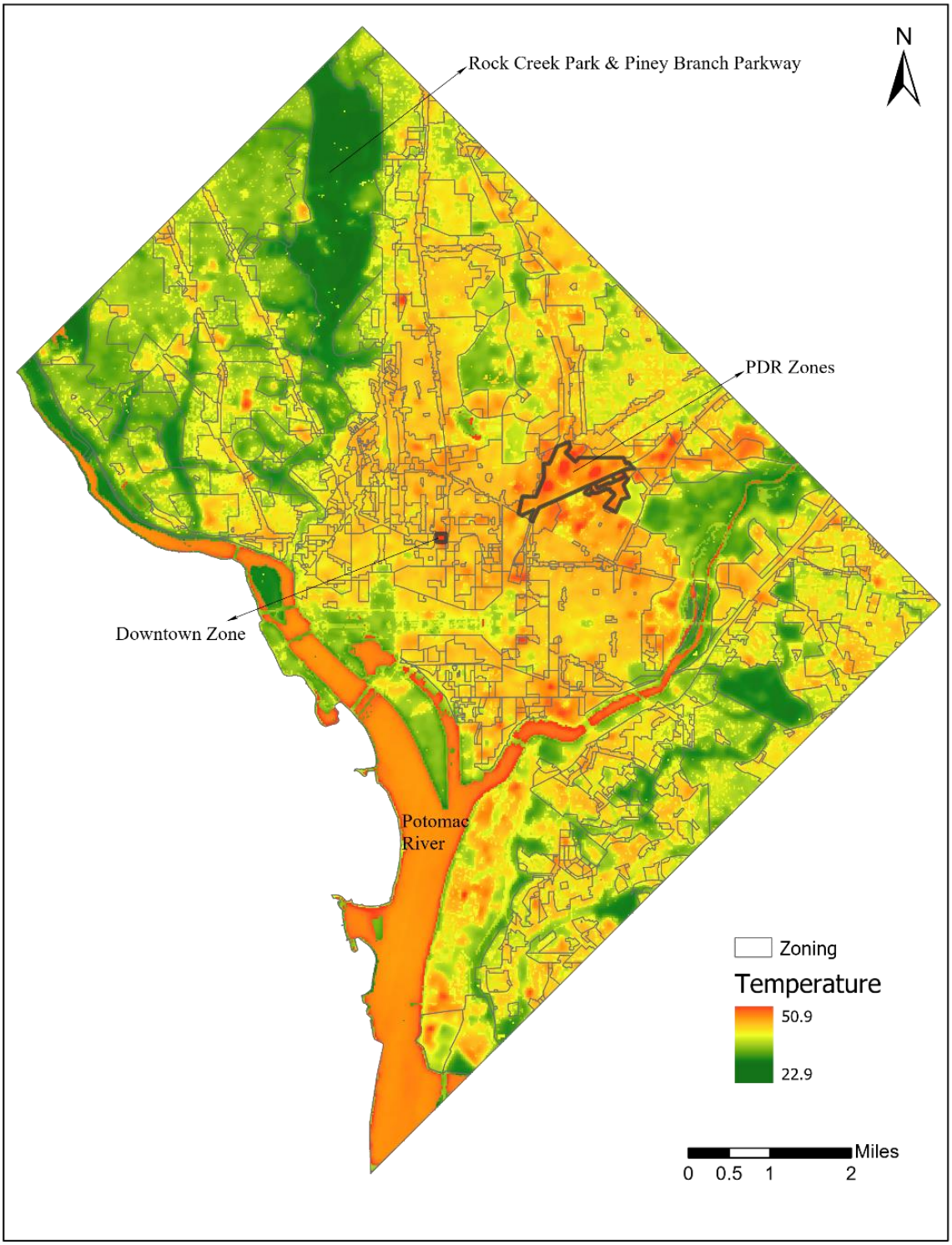

Figure 2. Washington D.C. heat map of July 27th, 2019.

After creating the city heat map, by using the same thermal image, I looked at the building rooftop temperatures for further analysis. Based on Best Management Practices data, there are records of 380 green roof buildings. But after I applied 0.25 NDVI as a criterion to select active green roofs, the result returned 156 buildings. The reason could be that on those buildings which were excluded, a small fraction of the building is covered by green stuff, therefore, the average NDVI for the whole rooftop is less than 0.25. As the result, I have 156 buildings with high percentages of green coverage on the rooftop. In Figure 3, there is an example of how the recorded green roofs are excluded in our selected data.

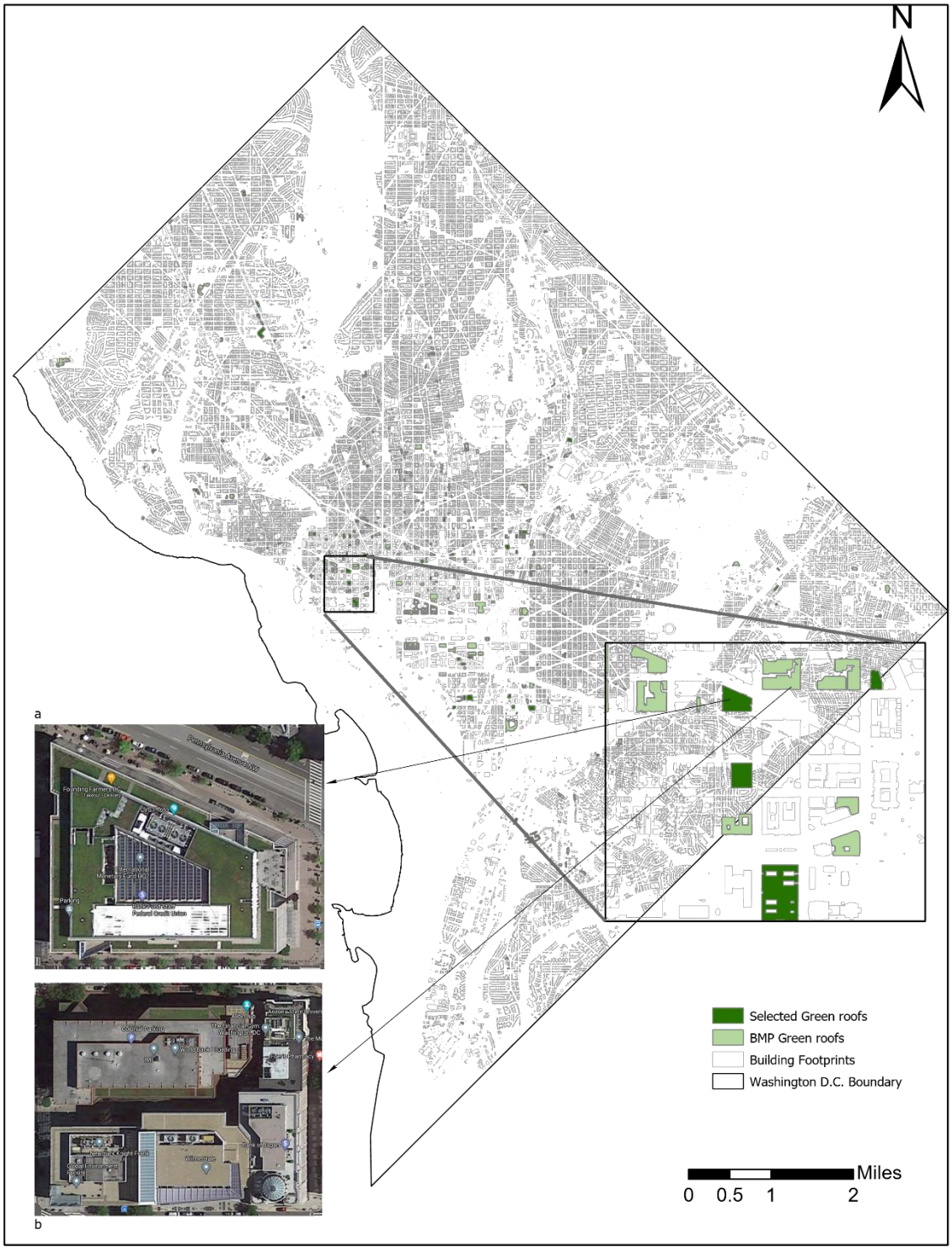

Figure 3.Selection of active green roofs. a) a building with a good coverage of green plants and NDVI value of > 0.25. b) A green roof building with small fraction of green plants on north side of it with NDVI value of < 0.25.

As mentioned before, the initial attempt to find the best match for the 156 green roofs among the more than 161,000 total buildings was not successful. Therefore, I used thresholds in Table 2 to narrow the number of conventional roof buildings which could be a match for green roofs.

Table 2: Selection of conventional roof buildings thresholds.

Criterion	**Value(s)**
Treatment	= 0
Mean-NDVI	< 0.25
Density of Buildings	0.14 < x < 50.86
Distance to green spaces	0 – 580 m
Area of buildings	28 – 24920 m^2
Building height	0 – 44 m

By applying the thresholds indicated in Table 2, 54,760 conventional roofed building were selected with characteristics matching those of green roofed buildings. Having a single table containing 54,760 conventional and 156 green roof buildings, I ran the MatchIt package in R to perform propensity score matching. By using the MatchIt package, I matched the most conventional roof buildings that were most similar to their green roof building counterparts. For running the code, I used “nearest” method, and used building height, distance to green space, building density, and building area to match buildings categorized as treatment 0 (conventional) by treatment 1 (green roof). The final 312 buildings (156 conventional roof buildings and 156 green roof buildings) were output to a csv file for later analysis.

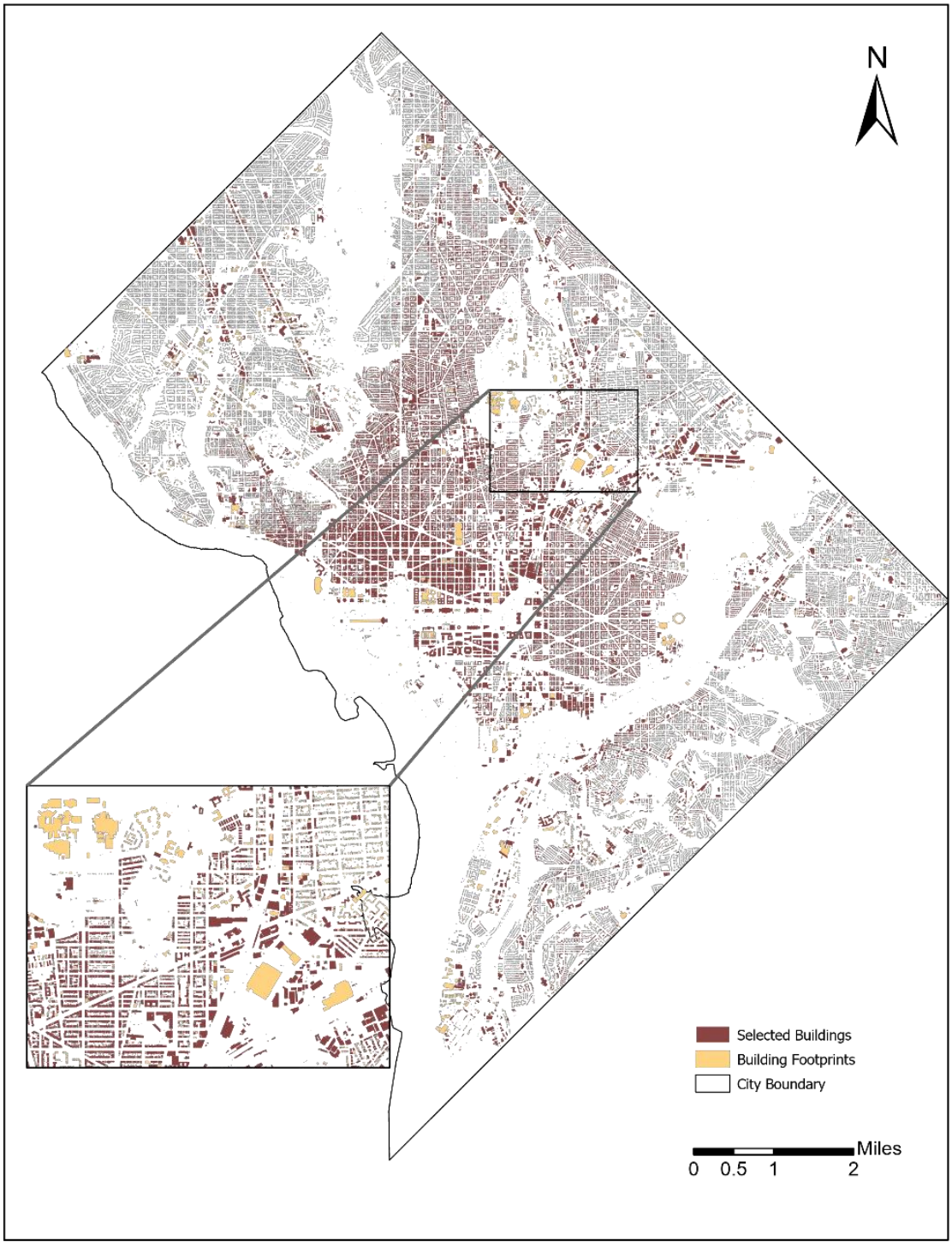

Figure 4. Selected buildings according to defined thresholds.

I used the Welch two-sample t-test for unequal covariance to compare the matched building rooftop temperatures and determine whether there is a significant difference between the means of two groups. Result show that green roofs are meaningfully cooler than conventional roofs. I determined the significance level as 0.05, therefore, by using two-tailed hypothesis, the result is significant at $p < 0.05$. The t-value is equal to 3.7913 and the p-value equal to 0.0001852 with 267.53 degree of freedom. Results show that the mean temperature of conventional roofs is 37.66˚C and 36.57 ˚C for green roofs. Although this temperature difference is only 1.09 ˚C, the t-test supports the argument that green roof temperatures are significantly lower than conventional roof temperatures. According to EPA "The annual mean air temperature of a city with 1 million people or more can be 1.8–5.4°F (1–3°C) warmer than its surroundings." Therefore, based on this result, I can claim that about 1.1 ˚C differences on rooftops temperature is significant.

3.4. Discussion

As the result of this research shows, the green roofs have lower temperature than conventional roofs. Also, the green areas in the heat map (Figure 2) have lower temperature within the city border. This result aligns with the other research which used either a model or a small experimental plant bed to talk about green areas effect on UHI. Based on Gill et al. (2007) covering a roof with as little as 10% green cover could reduce the surface temperature 7 - 8.2℃ in city of Greater Manchester as a high-density residential areas and town centers respectively by 2080, compared to a 1961-1990 baseline case. Alternatively, they said that if the green covered area of roofs stayed the

same, the temperature will increase by 3.3 – 3.9℃ in high-density residential areas and town centers, respectively, by 2080. Although I did not use a model in my research to predict the future temperature of the city in case of installing more green roofs, but the cooler temperature that green roofs provide could result in decrease in urban temperature.

In addition, Alexandri and Jones' (2008) said that the amount of vegetation placed on the buildings is very important. The all-green buildings, with both a green roof and green walls, play a more important role in decreasing the temperature. As I found in this research, rooftops with small fraction of green plants on them are not contributing to temperature reduction and they had very low NDVI value. Likewise, Susca et al. (2011) monitored UHI in four areas in New York City and found that there is an average of 2℃ in temperature differences between the most and the least vegetated areas. This temperature differences in current research is 1.1℃ over green and conventional roofs.

Simmons et al. (2008) said that because green roof performance varies, they need to be designed carefully to maximize their benefits in mitigating UHI. As I see in my data, the green roof temperature varies from 43.26 - 27.03 ˚C in the month of July. This could be because of many reasons like the type of green roof, the amount of plant planted on the roof, the green roof bed (if it is covered by white gravels or not), whether the rooftop is in the shade, I should also remind that I used 30m resolution satellite images for this study. Lastly, this study, as a pioneer to present data regarding the actual implementation of installing green roofs as an urban cooling strategy on a city scale, shows that the cooling effect of installing green roofs are significant.

Numerous studies have revealed that green roofs have the potential to cool urban environments. However, these studies have either been conducted on a small scale,

observing individual instances of cooling method application (Blanusa et al. 2013; Coutts et al. 2013; Köhler 2006; Ashraf Muharam, ElSayed Amer 2016; Simmons et al. 2008; Susca et al. 2011), or they have been attempts to model what would happen if such methods were adopted on a city or regional scale (Alexandri and Jones 2008; Khan and Asif 2017; J. K. W. Wong and Lau 2013). The result of this study is aligned with their finding by was derived using the data from the real world. Even though the thermal images had a relatively coarse resolution, they still confirmed that green roofs can reduce their surrounding surface temperatures.

3.5. Conclusion

This research looks at green roofs' potential for reducing the UHI. There are many benefits to green roof, which include, but are not limited to: enhanced aesthetic value, increased roof longevity, increase building value, stormwater runoff mitigation, potential of stormwater runoff quality improvement, air pollution reduction, noise reduction, decreased energy consumption, increased habitat for wildlife, and the ability to mitigate urban heat island effect (Santamouris 2014; Razzaghmanesh, Beecham, and Salemi 2016; Yang, Yu, and Gong 2008; Simmons et al. 2008; Li and Yeung 2014; Kalantar et al. 2017; Coutts et al. 2013; Wolf and Lundholm 2008; Kim 2004; Khan and Asif 2017; Ahmadi et al. 2015). Although many studies have estimated the cooling effect of green roofs by using small-scale in-situ data, but few studies (if any) have evaluated their performance under the context of remote sensing application in UHI, especially when integrated by analyzing real-world data. This study assessed the potential mitigation effects of green roof installations on selected green roof buildings in

Washington D.C. The result of this study confirmed the benefit of installing green roofs in reducing IUHI in Washington D.C. Therefore, other dense cities with similar characteristics like similar climate, green spaces within the city, urban density could expect to benefit from installing green roofs.

There were several limitations in conducting this research. For example, the coarse resolution of thermal images (30 m after resampling), using cubic convolution resampling (which estimates the temperature of each pixel by using a weighted average of 16 surrounding pixels). In a literature review research about methods and applications of TIR images for UH phenomenon, Weng (2009) emphasized that the scientific and user communities are looking forward to higher spatial resolution thermal images to have more accurate estimation of LST and emissivity. The proposed Hyperspectral Infrared Imager or HyspIRI mission has a TIR instrument with the spatial resolution of 60 m at nadir and a temporal resolution of 5 days (HyspIRI Team, 2018). The images from this satellite would allow for a slightly more accurate estimation of LST and emissivity than offered by current satellites. The HyspIRI instrument is still in the planning stages and until finer resolution thermal images become available, medium resolution Landsat and ASTER data will be the primary source of thermal imagery for UHI studies.

The satellite images were captured in the morning (11:46 a.m. EDT), where solar radiation might not have reached the ground in areas with high building. Also, the shade of building may underestimate the surface temperature in the thermal image. Since extensive green roofs can be retrofitted to existing roofs without the need for structural upgrade, they consider as a potential technique for urban heat mitigating strategy. The green roof contributes less to climate change than the conventional roof. Also, it needs

less replacement of building materials compare to both black and white roofs (Susca et al. 2011).

In the future research, I want to find out which month of the year is the month that green roofs have the highest effect on decreasing the rooftop temperature and also to compare the rooftops' temperature before and after green roof installation by using post-treatment analysis and demonstrate the changing pattern of the urban temperature as a result of the green roofs installation. I am expecting to find that green roofs can reduce the rooftop temperature in the warmest months of the year. Also, I am expecting to find a significant temperature differences before and after green roof installation in Washington D.C.

4. THE EFFECTIVENESS OF GREEN ROOFS FOR REDUCING ROOFTOPS TEMPERATURES SEASONALLY AND ANNUALLY

4.1. Introduction

In the Urban Heat Island phenomenon, the ambient temperature of an urban area is higher relative to its adjacent suburban and rural areas due to the thermal release of anthropogenic heat which is often exacerbated by a lack of green spaces and cool sinks. The Surface Urban Heat Island (SUHI) is defined as the difference between the surface temperatures within and without an urban area, and is an indirect UHI measurement method that examines the Land Surface Temperature (LST) using satellite images (Zhao, 2018). Thermal wavelengths measure the land surface temperature providing a spatially exhaustive measurement of LST which I use to conduct this UHI related research.

Because of urbanization and its attendant increase in concrete and other artificial surfaces, increasing the amount of green spaces in urban areas is an important mitigation technique for combating the UHI. Many urban areas, however, suffer from a lack of available free ground space on which to implement large scale UHI green spaces that mimic the environment before urbanization. But because of increases in building developments, roofs provide an excellent space to apply mitigation techniques (Santamouris, 2014). Akbari and Rose (2008) estimated that in four big cities in the US (Chicago, IL, Houston, TX, Sacramento, CA, and Salt Lake City, UT), 20% to 25% of the city is covered by roof surfaces. Therefore, rooftops provide a good area to apply urban heat mitigation techniques.

Two important goals to balance the thermal budget of cities are to increase thermal losses and decrease thermal gains. These goals seek to increase the urban environment albedo, develop green spaces in cities, and use natural heat sinks to absorb extra heat. These two goals for mitigating urban heat translate into two roof-related UHI mitigation techniques: the implementation of (a) cool or reflective roofs, which aim to increase roof albedo, and (b) green, or living, roofs, which cover the roof completely or partially with vegetation. Green roof design depends on many different factors, including thermal conductivity, specific heat, building density, thermal absorptance, solar absorptance, height of plants, and leaf area index. Besides mitigating urban heat, green roofs offer a variety of advantages like storm water retention, increased roof longevity, decreased energy consumption, better air quality and noise reduction, and the provisioning of space for wildlife (Kalantar et al., 2017; W. C. Li & Yeung, 2014; Razzaghmanesh et al., 2016; Santamouris, 2014; Simmons et al., 2008; Yang et al., 2008).

Many researchers identify three types of green roofs: intensive green roofs, semi-intensive green roofs, and extensive green roofs (medium depth of 2-20 cm, 12-100cm, and 15-200cm respectively) (e.g.: Li and Yeung 2014; Banting et al. 2005; Khan and Asif 2017; Ahmadi et al. 2015). Other researchers identify two types of green roofs: the extensive roof with a depth of less than 150 mm and the intensive roof with the depth of greater than 150 mm (e.g: Razzaghmanesh, Beecham, and Salemi 2016; Ashraf Muharam, ElSayed Amer 2016; Williams, Rayner, and Raynor 2010). Intensive green roofs, which can hold greater numbers of closely spaced plants could be more effective on heat reduction on rooftops.

As Dong et al. (2020) mentioned in their research, the season factor should be considered in further studies about green roof. In this research I analyzed the actual implementation of green roof installations as an urban cooling strategy on a city scale. More specifically, the first objective of this research was to examine monthly differences in the temperatures of green and conventional roofs to find out which months exhibited significant temperature differences. This analysis informed about the seasons when green roofs would provide the greatest potential reduction of the UHI. The second objective was to compare rooftop temperatures before and after green roof installation to further assess their influence on urban temperature and the UHI. Throughout this research I used the term intra-urban heat island (IUHI) to describe the temperature differences between the different sites within the city limits of Washington D.C.

Our first objective was to identify the month(s) when green roofs had their greatest impact on the ambient temperature. Our null and alternative hypotheses were:

Null hypothesis: There is no difference between green and conventional roof temperatures in different months.

Alternative hypothesis: Green roof temperatures are lower than conventional roof temperatures in certain months.

The second objective was to compare rooftop temperatures before and after green roof installation to further assess their influence on urban temperature and the UHI. Our null and alternative hypotheses were:

Null hypothesis: There is no difference in rooftop temperatures before and after green roof installations.

Alternative hypothesis: Rooftop temperatures are lower once green roofs are installed.

4.2. Data and Methodology

I collected Landsat 8 satellite images for all months of 2019 except February and June, and for one month in 2009. I repeated the steps described in Chapter 3 to process these images and convert them from a quantized digital number to a surface temperature expressed in degrees centigrade. I also obtained ancillary data including building footprints, roof types, building heights, and parks and green areas to answer our research questions. To fulfill the objectives of this study, I selected equal numbers of conventional and green roof buildings that had similar ancillary data characteristics. For the first objective, I used two-way ANOVA to compare the mean temperature differences between building type groups that have been split on two independent variables (months and roof type). For the second objective, I used linear regression to find out the relationship between rooftop temperature (dependent variable) and roof type (independent variable).

4.2.1. Study Area

The study area is Washington D.C., the capital of the United States of America. It is surrounded by the States of Maryland and Virginia with a total area of 68.34 mi^2 and a population of 681,170 according to the 2016 census. Based on the Köppen–Geiger climate classification, Washington D.C. has a "Humid Subtropical" climate, and the 2009 and 2019 average seasonal temperatures and the annual precipitation are shown in Table 3. (National

Weather Service- Washington D.C. temperature, 2020; National Weather Service-Washington D.C. Precipitation, 2020). Washington, D.C. is a compact city with more than 161,000 buildings.

Table 3: Temperature and precipitation record of Washington D.C.

Year	Temperature (˚F)					Precipitation (in)
	Winter	Spring	Summer	Autumn	Annual	Annual
2019	39.5	60.1	79.5	62.2˚	60.6	42.34
2009	37.3	55.9	76.8	60.3	57.4	46.9

4.2.2. Data

The primary dataset for this study was the thermal bands of Landsat 8 imagery from which I calculated the land surface temperature in degrees centigrade (see Chapter 3). Additional PlanetScope imagery was obtained from Planet Inc (Planet Labs, 2019) to facilitate the identification of green roof buildings. PlanetScope imagery has four spectral bands (Blue, Green, Red and Near-Infrared) with an approximate spatial resolution of 4 meters. I also used several datasets provided by the City of Washington, D.C. on their open data website (https://opendata.dc.gov/), including the following geospatial and tabular datasets: the city boundary, building footprints, the Best Management Practices (BMP) report, national and city park and recreation boundaries, and a normalized Digital Surface Model (nDSM) that separately identified surface and ground features. Using these datasets, I calculated several variables that influence rooftop temperatures in addition to the presence or absence of green roofs.

The BMP dataset described structural controls used to manage stormwater runoff including the identification of green roof buildings, but I found that some buildings were erroneously identified. Buildings that had an average rooftop NDVI greater than 0.25 were identified as actual green roof buildings. I calculated the average height of each building

from the nDSM using zonal statistics. I calculated the Euclidean distance of each building from its nearest green area (e.g. park) using the NNJoin package in QGIS (NNJoin 3.1.3 documentation, 2018). Building density was calculated as the percentage of a 170 meter buffer surrounding each building that was covered by building footprints. The 170 meter buffer size was selected because it was slightly larger than the average building footprint area of 160 m^2 and so the highest building density will approach 100%.

4.2.3. Land Surface Temperature (LST) Retrieval

For the first objective, Landsat 8 images were obtained from the USGS EarthExplorer website for each month of 2019 except February and June, for which there are no cloud-free images available. A Landsat 5 TM image from May 12, 2009 was also obtained from the USGS website to complete the second objective. Landsat 8 images have two thermal bands from the Thermal Infrared Radiometer (TIRS) sensor corresponding to 10.60 – 11.19 µm (Band 10) and 11.50 - 12.51 µm (Band 11) wavelengths. The thermal measurements are made at 100-meter spatial resolution, but the data is resampled using cubic convolution and the product is delivered as 30 meter pixels. In Landsat 5 TM, band 6 is the thermal band corresponding to 10.40 - 12.50 µm wavelength with the resolution of 120 m before resampling.

Raw Landsat 8 thermal imagery needs to be converted to actual surface temperatures through the same processing steps described in chapter 3. The only extra step in this conversion process is to convert Landsat 5 DNs to spectral radiance by using the equation below:

$$L_\lambda = \text{Grescale} * \text{QCAL} + \text{Brescale}, \quad (1)$$

Where L_λ = Spectral Radiance at the sensor's aperture in watts/(meter squared * steradian * μm), Grescale = Rescaled gain (the data product "gain" contained in the Level 1 product header or ancillary data record) in watts/(meter squared *steradian * μm)/DN, Brescale = Rescaled bias (the data product "offset" contained in the Level 1 product header or ancillary data record) in watts/(meter squared *steradian * μm). Once converted to at-sensor spectral radiance, the process outlined in Chapter 3 for converting to surface temperature in degrees centigrade was followed.

4.2.4. Comparing Buildings with Similar Characteristics: Propensity Score Matching

Using the processed thermal images for the 10 cloud-free months of 2019, I calculated the minimum, maximum, and mean temperatures for all building rooftops to compare temperature differences between green and conventional roofs. Based on the BMP and NDVI data, I identified 156 active green roof buildings in Washington D.C. among more than 161,000 buildings. To make appropriate temperature comparisons between green and conventional roofs, I needed to ensure that other building characteristics were as similar as possible between buildings. For example, I did not want to compare the temperature of a small, short, green roof building that was close to a green space with the temperature of a large, tall, conventional roof building that was far from any green space. The building attribute data (Table 4) was input into a propensity score matching routine found in the R MatchIt package to select a conventional roof building that had similar characteristics to every green roof building. The MatchIt output was optimized by limiting the search of possible matches to those buildings within the ranges shown in Table 4.

Table 4: Selection of conventional roof buildings thresholds.

Criterion	Value(s)
Treatment	= 0

Mean-NDVI	< 0.25
Density of Buildings	0.14 < x < 50.86
Distance to green spaces	0 – 580 m
Area of buildings	28 – 24920 m^2
Building height	0 – 44 m

By using the above threshold values, I reduced the number of potentially matching conventional roof building from ~161,000 to 54,760. This reduced set of buildings and the 156 green roof buildings yielded a total of 54,916 buildings for the MatchIt propensity score matching routine. The output was a list of the 156 conventionally roofed buildings that most closely matched the 156 green roofed buildings.

4.2.5. Monthly Rooftop Temperature Differences: Two-way ANOVA

The primary purpose of a two-way ANOVA is to understand if there is an interaction between the two independent variables on the dependent variable. In order to determine if a seasonal IUHI exists, I compared seasonal differences in defined pairs (as the output of the MatchIt routine) of green roofs and conventional roofs via a two-way ANOVA to compare the mean temperature (dependent variable) of green roof and conventional roof buildings, where roof type is independent variable one or factor one with two values (0 = conventional roofs and 1= green roofs) for each month (independent variable two/ factor two with 10 values). The results of that test reveals whether the month of the year interacts with roof type to give rise to mean differences in rooftop temperatures. In the event such an effect was detected, Tukey post-hoc test pinpointed the month or months in which statistically significant differences exist in mean roof temperature by roof type (green vs. conventional).

4.2.6. Rooftop Temperatures Before and After Green Roof Installation: Difference in Difference Linear Regression

In this section I aim to test for differences in rooftop temperature before and after installation of a green roof. I select 2 periods that were enough years apart that there was a sizable number of buildings that had transitioned to green roofs. Based on the Department of Energy & Environment (DDOE) data, green roof database, the first green roof building was installed in 1975 and by 2005 there were less than ten installed green roofs in Washington D.C. (Figure 5). In 2009 the number of green roofs had increased to 89. I chose 2009 to compare with 2019 because the number of green roofs had increased and there was a large enough number to compare to 2019. Although the "Green Building Information Gateway" website shows 89 green roof buildings in its collection, only 9 of them were included in the 2019 green roof data. While the reasons for this discrepancy are not clear, it could be that the portion of the roof with green stuff coverage was so low that its NDVI value was less than our defined threshold.

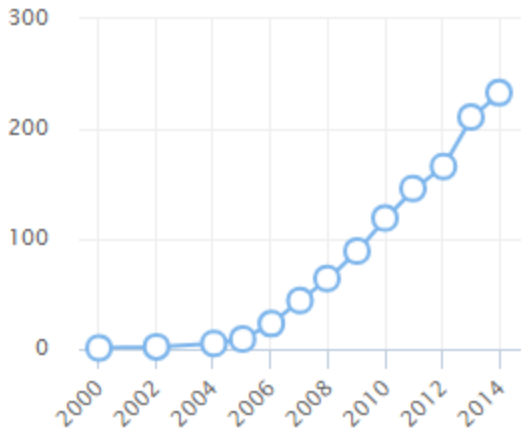

Figure 5. Cumulative green roof installation in Washington D.C. (Source: GBIG, 2018. http://www.gbig.org/collections/14619)

Based on the result of first objective, I selected the month that green roofs show significant difference in the temperature for each year compared to conventional roofs. For this purpose, I used Landsat 5 images for May 2009 and Landsat 8 for May 2019 data (Landsat 7 was malfunctioning in 2009). There is no doubt that for 10 years there are many factors that can change the temperature of the rooftop besides installing green roofs—factors like air temperature, land uses, and/or impervious surface cover. I used a difference-in-differences approach, specifically, propensity score matching to select a "control group" of buildings that are most similar to the 156 green roof buildings with respect to attributes such as size, floor area, building height, distance to selected land uses, surrounding building density. I needed to select the very same buildings in 2009 to be able to compare their temperature. Among 156 green roof building, only 144 buildings existed in 2009 and only 8 of them had green roof on their rooftops. Therefore, I have a spreadsheet containing 576 records; two sets of 144 buildings (2019 green roofs, and 2019 conventional roofs), eight common green roof buildings in 2009, 136 conventional roof buildings that converted to green roof over ten years, and 144 common conventional roofs in 2009. From there, I then used linear regression to detect and evaluate the significance of any "treatment effect," or mean effect on roof temperature, due to the installation of green roofs:

$$Y = \alpha + \beta 1\ \text{Time} + \beta 2\ \text{Treatment} + \gamma\ \text{Time*Treatment}, \quad (2)$$

Where Y is building roof temperature, Time is an indicator variable that takes on a value of 0 if an observation was made in 2009 and 1 if the observation was for 2019. Treatment is another indicator variable that takes on a value of 1 if a building has a green roof and a value of 0 if the building is part of the propensity score selected "control group", and

Time*Treatment is an interaction between the two indicator variables. The null hypothesis is that γ, the slope parameter on the interaction effect, is equal to zero. The alternative is that the parameter is nonzero. In statistical parlance, the parameter represents the "difference-in-differences" between the green roof buildings and the control group of buildings. That is, it represents the arithmetic difference between two terms: (1) the end period (2019) difference in mean roof temperature between green roof and conventional roof buildings; and (2) the beginning period difference in mean roof temperature between the two building types. In other words, the parameter estimates for γ obtained via least squares regression is equal to:

$$\hat{\gamma} = d_2 - d_1 \tag{3}$$

Where, $d_1 = \mu T_{G2009} - \mu T_{C2009}$, and $d_2 = \mu T_{G2019} - \mu T_{C2019}$, μT is the mean temperature value.

Formally, the null hypothesis of the test is: $H_0 = d_2 - d_1 = 0$

The null hypothesis can be evaluated using the t-statistic associated with the partial regression coefficient, or parameter estimate, $\hat{\gamma}$ obtained from estimating the regression equation specified above. In the event that the parameter estimate takes on a negative, statistically significant value, the model will detect a meaningful "treatment effect," whereby installing green roofs is linked to reduction in mean roof temperature that cannot be explained by chance alone.

Finally, I have a table contains 144 green roofs in 2019 (Time= 1, Treatment= 1), 144 conventional roofs in 2019 (Time= 1, Treatment= 0), 8 green roofs in 2009 (Time= 0, Treatment= 1), and 280 conventional roofs in 2009 (Time= 0, Treatment= 0).

Afterwards, I run the linear regression code in R to find the relationship of treatment and temperature over 10 years of green roof installation.

4.3. Results

For the first objective, the results (Table 5) show the p-value for month, treatment, and month-treatment combination, is less than 0.05 which means there are differences in the means in groups. Therefore, both month and treatment (installing green roof) are significantly related to the roof temperature.

Table 5: Two-way ANOVA result

	Df	Sum Sq	Mean Sq	F value	Pr (>F)
Treatment	1	271	271	92.941	< 2e-16
Month	9	872183	96909	33276.175	< 2e-16
Treatment:Month	9	144	16	5.506	1.51e-07
Residuals	3100	9028	3		

And below is the Tukey pos-hoc test result:

Table 6: Tukey pos-hoc test result

Treatment	Temperature mean difference	lower confidence interval at 95%	upper confidence interval at 95%	p-value after adjustment
T1-T0	-0.59	-0.71	-0.47	0

In table 6, “T” stands for treatment where T1 is green roof and T0 is conventional roof. In table 6, it can be seen from the output, that time pairs comparisons are significant with an adjusted p-value < 0.05. There is a -0.59 ˚C differences in temperature before and after installing green roofs, which indicated that installing green roofs have decreased the rooftop temperature by 0.59 ˚C.

Discussing Tukey pos-hoc result table, I need to compare the pairs which have the same month but different treatment where the p-value is less than 0.05. Table 7 is showing these pairs that have differences in temperature before and after treatment.

Table 7: Summary of Tukey pos-hoc test for comparable pairs.

Treatment/Month	Temperature mean difference	lower confidence interval at 95%	upper confidence interval at 95%	p-value after adjustment
T1:Jan-T0:Jan	-0.04	-0.73	0.65	1.0000000
T1:Mar-T0:Mar	-0.35	-1.04	0.33	0.9571733
T1:Apr-T0:Apr	-0.36	-1.05	0.32	0.9432984
T1:May -T0:May	-1.09	-1.77	-0.40	0.0000039
T1:Jul -T0:Jul	-1.09	-1.77	-0.40	0.0000039
T1:Aug -T0:Aug	-1.05	-1.74	-0.37	0.0000102
T1:Sep-T0:Sep	-0.67	-1.36	0.01	0.0600855
T1:Oct -T0:Oct	-1.05	-1.74	-0.37	0.0000102
T1:Nov-T0:Nov	-0.18	-0.87	0.50	0.9999929
T1:Dec-T0:Dec	0.00	-0.69	0.69	1.0000000

As shown in the highlighted rows in table 7, the temperature on green roofs are lower than conventional roofs by 1.08, 1.08, 1.05, 1.05 ˚C respectively in months May, July, August, and October where the p-value is less than 0.05. Washington D.C. weather (National Weather Service- Washington D.C. temperature, 2020) shows that in 2019, from May to September the average monthly temperature was 70+ ˚F, which indicates them as the warmest months of the year 2019. As the results show, we see the temperature differences on green rooftops and conventional rooftops during these warm months. As I mentioned earlier, there is not a cloud-free image for the month of June 2019. Also, the Tukey pos-hoc test does not return a significant temperature differences in the month of September. Generally, we can see the pattern that green roofs temperature are cooler than conventional roofs in the warm months of the year in 2019. Although the differences are only about 1 ˚C, but considering that the international effort is to attempt to limit global warming to 1.5 °C above pre-industrial levels (King & Karoly, 2017) and according to the EPA “The annual mean air temperature of a city with 1 million people or

more can be 1–3°C warmer than its surroundings", I can claim that the 1 ˚C differences could be significant in IUHI.

Because I need to compare the rooftops temperature from the same month in years 2009 and 2019 for objective two, I refer to the result of the first objective and choose one of the four months with significant temperature differences. Among those four months, there are only could-free images for May and August. Since May is one of the greenest months of Washington D.C., I chose the satellite image of May 2009 and compared it with thermal image of May 2019.

For the second objective I used linear regression to find out the temperature differences between before and after green roof installation. Results are reported in Table 8.

Table 8: May 2009-2019 Linear Regression result

	Estimate	Std. Error	t value	Pr (>|t|)
(Intercept)	32.77	0.33	100.38	< 2e-16
Time	-2.49	0.56	-4.45	1.05e-05
Treatment	1.26	1.96	0.64	0.52
Time:Treatment	-2.29	2.06	-1.11	0.27

Residual standard error: 5.522 on 590 degrees of freedom
Multiple R-squared: 0.0707, Adjusted R-squared: 0.06598
F-statistic: 14.96 on 3 and 590 DF, p-value: 2.126e-09

In the above result, it can be seen that p-value of the F-statistic is 2.126e-09, which is highly significant. This means that, at least, one of the predictor variables is significantly related to the outcome variable. It can be seen that "Time" is significantly associated with the temperature where its p-value is less than 0.05. The coefficient for Time:Treatment is the differences in differences estimator. Although the effect of treatment is not significant (p-value > 0.05), the treatment has a negative effect which means that installing green roof could reduce the rooftop temperature.

Based on the above result the model equation can be written as follow:

Temperature = 32.77 - 2.49*Time + 1.26*Treatment – 2.29*Time*Treatment

As the above results show, although treatment caused reduction in temperature, it does not show a significant relationship with the it. As Table 8 is shows, the p-value of treatment is not significant which means I cannot claim that installing green roofs have decreased rooftop temperatures during these years. There are good reasons why I don't have a solid result that aligns with the expectation and the number of samples in 2009 (8 green roofs) is the main reason for it. Four buildings out of the eight green roof buildings in 2009 has relatively small areas which could result in not having a robust cooler degree on their rooftop compare to matched conventional roofs. Moreover, it is important to mention that the majority of the 8 green roofs were less than two to three years old and so were not fully operational leaving exposed some soil medium led to higher rooftop temperatures. This fact could explain more why the result of differences in differences linear regression is not significant. Unfortunately, these results are not expected results and based on them I cannot claim that installing green roofs have reduced the temperature of the rooftops over years.

4.4. Discussion and Conclusion

This study discussed the potential mitigation effect of green roofs on seasonal building temperatures in Washington D.C. According to several scientific studies on small samples of green roof materials (Simmons et al. 2008; Susca et al. 2011), installing green roofs can reduce the rooftop temperature. Our results for the first objective are aligned with their findings and confirm that green roofs are cooler than conventional roofs during warm months of the year when the IUHI is more pronounced. While it is not known if the pattern would hold true for the month of June, since there were no cloud-

free images in June 2019, that May and July demonstrated significantly higher temperatures it may be assumed that June would have also. Also, the p-value for September was not less than 0.05 but it is close enough (0.06) that I can generalize the result to the six warm months of the year (May-October). The uniqueness of this research is that this is the first research I am aware of that compares actual rooftop temperatures across a city by using the satellite images applied to the real cases of green roof buildings.

Even though the results show that green roofs are only effective May-October for cooling purposes, we should remember that even in cold weather they could be a great insulation system to reduce energy consumption for building heating purposes. Green roofs are considered a passive strategy to reduce energy consumption in different climates by working as insulation. The energy saving performance of green roofs depends on climatic conditions, building function, insulation of the building envelope, and the type of green roof. While green roofs provide shade, insulation, and evapotranspiration against solar radiation, they also reduce the indoor air temperature in summer. During winter, green roofs act as wind shields and reduce heating loads, but the temperature regulating effect during winter is less than in summer (Khan & Asif, 2017).

Although the result for the second objective was not desirable, we should consider the quality of availability data that I had for this research. The thermal images from Landsat 5 and 8 that I have used have the resolution of 30m after resampling (120 m and 100m before resampling, respectively), which are the best freely accessible thermal images available, but which are not ideal for studying small rooftop areas. In addition, the cubic convolution resampling method used to create the 60-meter resolution images

makes the temperature for each pixel an estimation from its 16 surrounding pixels, which again affect the recorded temperature. Besides the coarse resolution of the images, having a small sample (only eight buildings) which had small areas and have a relatively new green roofs installed, could have affected my results. Therefore, I can say that there still may be the temperature differences from 2009 to 2019 because of installing green roofs, but I could not confirm them by using these satellite images.

In our data, the temperature range on green roof in May 2019 is from 20.49 to 33.76 ˚C and this range is from 23 to 44.7˚C in May 2009. There are many factors that influence the green roofs' temperature. For instance, the type of green roofs and the plants can affect the cooling effect very much. As Simmons et al. (2008) suggest, because green roof performance varies, they need to be designed carefully to maximize their benefits in mitigating the UHI.

Santamouris (2014) indicated that the season could paly a role in the intensity of the UHI and the findings in this chapter confirmed that is the case. The intensity of the UHI tended to be higher during warm months of the year and lower during cooler months (Schatz & Kucharik, 2014). These findings indicate the cooling effect of green roofs were most significant during warm months. According to other studies on green roof which were conducted on small scale samples, green roofs perform differently in different seasons. The finding of this research confirmed that installing green roofs can positively impact rooftops to have cooler temperatures during warm months of the year. It is recommended to investigate more in installed green roofs with a finer resolution thermal images if available in the future.

5. EXAMINATION OF THE URBAN HEAT ISLAND VIA CITY-WIDE INSTALLATION OF GREEN ROOFS

5.1. Introduction

The Urban Heat Island (UHI) is characterized by the development of higher temperature in cities compared to their surroundings. When the study area is limited to a city border, it is called Intra-Urban Heat Island (IUHI). There are different techniques to mitigate this phenomenon and choosing a proper mitigation strategy is directly related to the existing surface condition of that city (Hashem Akbari & Rose, 2008; Mohajerani, Bakaric, & Jeffrey-Bailey, 2017). A few strategies to reduce the city temperature include using white roofs and walls, installing green roofs, increasing green lands and parks. As the consequence of urbanization and the replacement of green areas by impermeable surfaces, the available free ground area in the urban environment on which to implement large scale UHI mitigation techniques are very limited and the proportion of land dedicated to plants and trees is smaller than before urbanization. At the same time, because of increases in building developments, roofs provide an excellent space to apply mitigation techniques (Santamouris, 2014).

Green, or living, roofs, cover the roof completely or partially with vegetation. The vegetation of green roofs is grown in a soil medium over a waterproofing membrane. Beneath the soil layer, there is a filter that prevents soil from washing away. The last layer is a water proofing membrane to protect the roof. Green roofs reduce the roof top surface temperature as well as ambient air temperature due to the roof's thermal benefits, including the insulating effect of the soil substrate and vegetation, the shading from the

plant canopy and transpirational cooling. Besides mitigating urban heat, green roofs offer a variety of advantages like storm water retention, increased roof longevity, decreased energy consumption, better air quality and noise reduction, and the provisioning of space for wildlife (Kalantar et al., 2017; W. C. Li & Yeung, 2014; Razzaghmanesh et al., 2016; Santamouris, 2014; Simmons et al., 2008; Yang et al., 2008).

The Toronto, Canada city council adopted "Toronto's Green Roof Strategy" in 2006 to encourage increased green roof construction within the city. This strategy was based on a study which indicated that widespread implementation of green roofs in Toronto would provide significant economic benefits to the City, particularly in the areas of stormwater management and reducing the urban heat island and the associated amount of energy used for cooling. In 2010, the City of Toronto Green Roof Bylaw was passed which required and governed the construction of green roofs. This bylaw "supports the implementation of city-wide environmental policy objectives of the Climate Change, Clean Air and Sustainable Energy Action Plan, Transform TO and the Wet Weather Flow Management Master Plan. The City's Official Plan also supports the use of green roofs as an innovative approach to reducing the urban heat island effect in Toronto" (Toronto, 2020). After adoption of the Green Roof bylaw by the City of Toronto, it became the first city in North America to both require green roofs and establish construction standards for them. This bylaw requires 20-60% green roof installations on new developments or additions that are greater than 2,000 m^2 in gross floor area (City of Toronto, 2012). Six-hundred and twenty green roof projects were permitted by 2018 and 500,000 m^2 of green roof were installed from 2009-2018. "Annual benefits of the bylaw include 222 million liters of stormwater retained, 225 tons of carbon sequestered, 3.2 KWH of direct

electricity savings and more than 1,600 jobs" (Pecks S.W., 2019). In this research I apply the City of Toronto bylaw criteria to possible a green roof scenario in Washington D.C. and examine their impact on the IUHI.

In this research I defined two scenarios to select buildings and apply green roof temperatures to them to examine the effect on the broader IUHI. Other research has used different models to stimulate the UHI in a city by providing parameters and run the model. But in this research, I want to see what the effects of widespread green roof implementation would be. In our previous research, I calculated the green and conventional rooftop temperature differences, and in this research, I use them to find out if the application of green roofs on a subset of all the buildings in Washington D.C. would make a difference to the IUHI.

To examine the large-scale potential of green roofs to mitigate the IUHI, I calculated and visualized total reductions in temperature by artificially applying green roofs to a defined portion of buildings in Washington D.C. to model two hypothetical UHI scenarios:

a) Installation of green roofs on 10% of buildings in each Washington D.C. ward by using specific criteria for selecting buildings.

b) Installation of green roofs on building rooftops in accordance with the City of Toronto green roof bylaw policy.

5.2. Data and Methodology

To conduct our research, I gathered building footprint, building height, parks and recreation areas, impervious surface, and green roof buildings from the DC.gov website. I used PlanetScope satellite imagery to calculate NDVI for selecting active green roof buildings. I used building footprints and the number of above-ground floors in a building to calculate gross floor area. I collected Landsat 8 thermal images for May 24th, July 27th, August 12th, September 29th, and October 15th of 2019, and January 19th of 2020 from the USGS EarthExplorer website. Raw Landsat 8 thermal imagery was converted to actual surface temperatures by following the steps in chapter 3. Based on my previous findings, buildings with green roofs installed had lower rooftop temperature than conventional rooftop buildings in May, July, August, and October. I accounted for uncertainty in the cooling effects of hypothetically installed green roofs by randomly selecting temperatures from the lower and upper 95% confidence intervals (Table 9) and applying those temperature reductions to conventional rooftop temperatures. The hypothetically applied green roofs were then rasterized and combined with the corresponding thermal image. This green roof-based thermal image was then stratified into impervious and pervious surface categories, and the average temperature difference between impervious and pervious was calculated as the IUHI.

The configuration of green areas in a city can be as important as the size of the green areas in reducing the ambient temperature (Asgarian et al. 2015; Maimaitiyiming et al. 2014). The first scenario of hypothetical green roof installations is to apply the green roof temperatures to 10% of the buildings in each city ward. I used wards to group the buildings in the aim of having an equal distribution of buildings across the city. I defined

10% as the threshold of hypothetical green roof installation since only about 10% or less of buildings in each ward matched our building selection criteria. I selected among conventional roof buildings that were located in the densest part of the ward and farthest distance from the existence green areas because these buildings would likely have the greatest impact on IUHI temperatures. Considering the City of Toronto bylaw, I selected buildings with height greater than 6 meters. Because of Washington D.C. restrictions, there is no building higher than 34 m (except Cairo Hotel) within the city. There are 8 wards in Washington D.C. I defined several criteria for selecting buildings as listed below:

a. Buildings with conventional roofs

b. Building height between 6 - 36 m (3-12 floors), which defines low-rise buildings.

c. A building's gross floor area should be greater than 500 m^2.

d. Buildings should be in the densest part of the ward.

e. A building's distance to the green areas should be the farthest.

According to my previous study (Chapter 4), in the warm months of the year (excepting June for which there was not a cloud-free image), there are significant temperature differences between green and conventional roof buildings. I used these temperature differences (Table 9) to calculate hypothetical green roof temperatures and applied them to the selected building rooftops. Based on previous findings, the temperature on the rooftops were not significantly different in the month of September, but its p-value (0.06) is close enough to the margin (0.05) that I considered September in this analysis. I also examined the temperature differences in the month of January where

there are no significant differences between conventional and green rooftop temperatures as reported in the previous study.

The actual Landsat-based surface temperature of buildings in each of the months was the temperature recorded in the building attribute table as extracted from the thermal imagery for that period. Then, randomly selected values from within the lower and upper 95% confidence intervals (Table 9) was subtracted from the actual rooftop temperatures to calculate hypothetical green roof temperatures for the selected buildings. Because the values subtracted from the actual rooftop temperatures were drawn from the ranges identified by the lower and upper 95% confidence intervals, they are a measure of the confidence that should be attributed to the findings. The impervious surface vector layer including the hypothetical green roof buildings was then created and rasterized to create a new surface temperature map of Washington D.C. which will be used in the next step to examine the IUHI.

Table 9: Mean temperature differences of green and conventional roof buildings, GR= Green Roof, CR= Conventional Roof.

Roof type/Month	Temperature mean difference	lower confidence interval at 95%	upper confidence interval at 95%
GR:Jan-CR:Jan	-0.03	-0.73	0.65
GR:May -CR:May	-1.09	-1.77	-0.40
GR:Jul -CR:Jul	-1.09	-1.77	-0.40
GR:Aug -CR:Aug	-1.05	-1.74	-0.37
GR:Sep-CR:Sep	-0.60	-1.36	0.01
GR:Oct -CR:Oct	-1.05	-1.74	-0.37

For scenario two, I used a modified version of the Toronto bylaw and applied it to Washington D.C. The modification to the Toronto bylaw was to apply green roof temperatures that did not meet the height criteria because Washington D.C. has limited building heights to 27 meters for residential buildings and 34 meters for businesses, or the width of the street in front of the building, whichever is smaller. Considering this

district rule for building heights, I selected from all Washington D.C. buildings with at least 3 floors and with gross floor areas greater than 2000 m^2. I then subtracted the green roof temperature differences to the corresponding percentages of the selected roofs (according to Table 10) to examine the IUHI temperature changes resulting from this scenario.

Table 10: Toronto Green Roof Bylaw table.

Gross Floor Area (Size of Building)	Coverage of Available Roof Space (Size of Green Roof)
2,000-4,999 m²	20%
5,000-9,999 m²	30%
10,000-14,999 m²	40%
15,000-19,999 m²	50%
20,000 m² or greater	60%

Across Washington D.C. there are 4,104 buildings out of 158,370 with a gross floor area greater than 2000 m^2, and a number of floors greater than or equal to 3. I used lower and upper confidence interval at 95% from Table 9 to randomly generate temperature difference for each selected building. Then I used these values for each selected building in the attribute table and applied it to the appropriate percentage of the rooftop to calculate each building's hypothetical green roof temperature. I repeated the process of calculating hypothetical temperature by using lower and upper interval values in table 9 to calculate the hypothetical temperature lower and upper intervals. The building vector layer of hypothetical green roof buildings was rasterized to create a new surface temperature map of Washington D.C. which was used in the next step to examine the IUHI.

The IUHI is more than the temperatures of green roofs and conventional roofs. And while a sizable component of urban infrastructure, buildings (and their roofs) are only one component of that infrastructure. An Urban Heat Island is, by definition, the temperature difference between regions inside an urban area and regions outside an urban area. This research has examined Washington D.C.—a single city without surrounding "rural" areas. Other researchers have used the term Intra-Urban Heat Island to describe this type of situation where the difference in temperatures must be made between green areas inside a city and the remaining "urban" area. In this research on Washington D.C., areas defined as impervious cover by city datasets were selected to be the "urban" areas and areas defined as pervious cover were selected as the "rural" areas. The two rasterized, hypothetical green roof scenarios described above are divided into impervious (urban) and pervious (rural) regions to calculate the IUHI before and after hypothetical green roof installation. Results indicate the effect new installations of green roofs would have on mitigating the IUHI in Washington D.C.

5.3. Result and Discussion

Table 11 shows the number of existing buildings in each ward and the number of buildings that receive a hypothetical green roof temperature.

Table 11: Number of Buildings in each ward.

Ward	Total No. of Buildings	10% of existing buildings	Existing Green roofs	No. of Buildings to convert Temperature	Matched buildings with criteria
1	12444	1244.4	17	1227	1227
2	11687	1168.7	27	1140	1140
3	21294	2129.4	32	2097	2097
4	29516	2951.6	13	2939	1818
5	26322	2632.2	10	2622	1553
6	23269	2326.9	47	2280	1613

7	22316	2231.6	5	2227	1386
8	14664	1466.4	5	1461	1461

I applied all criteria to select conventional roof buildings in each of the eight wards. Wards 1, 2, 3, and 8 have more matched buildings than 10% of it. Therefore, I selected the top 10% of buildings that are in the densest part of the city and are farthest from green spaces. I found that wards 4, 5, 6, and 7 had insufficient buildings to meet the 10% of all buildings' criterion. I therefore selected all matching buildings on which to apply a hypothetical green roof. That is, 6.2%, 5.9%, 6.9% and 6.2% of all buildings were used for wards 4, 5, 6 and 7, respectively. Figure 6 shows the distribution of the buildings that matched the criteria and received a hypothetical green roof temperature in each ward.

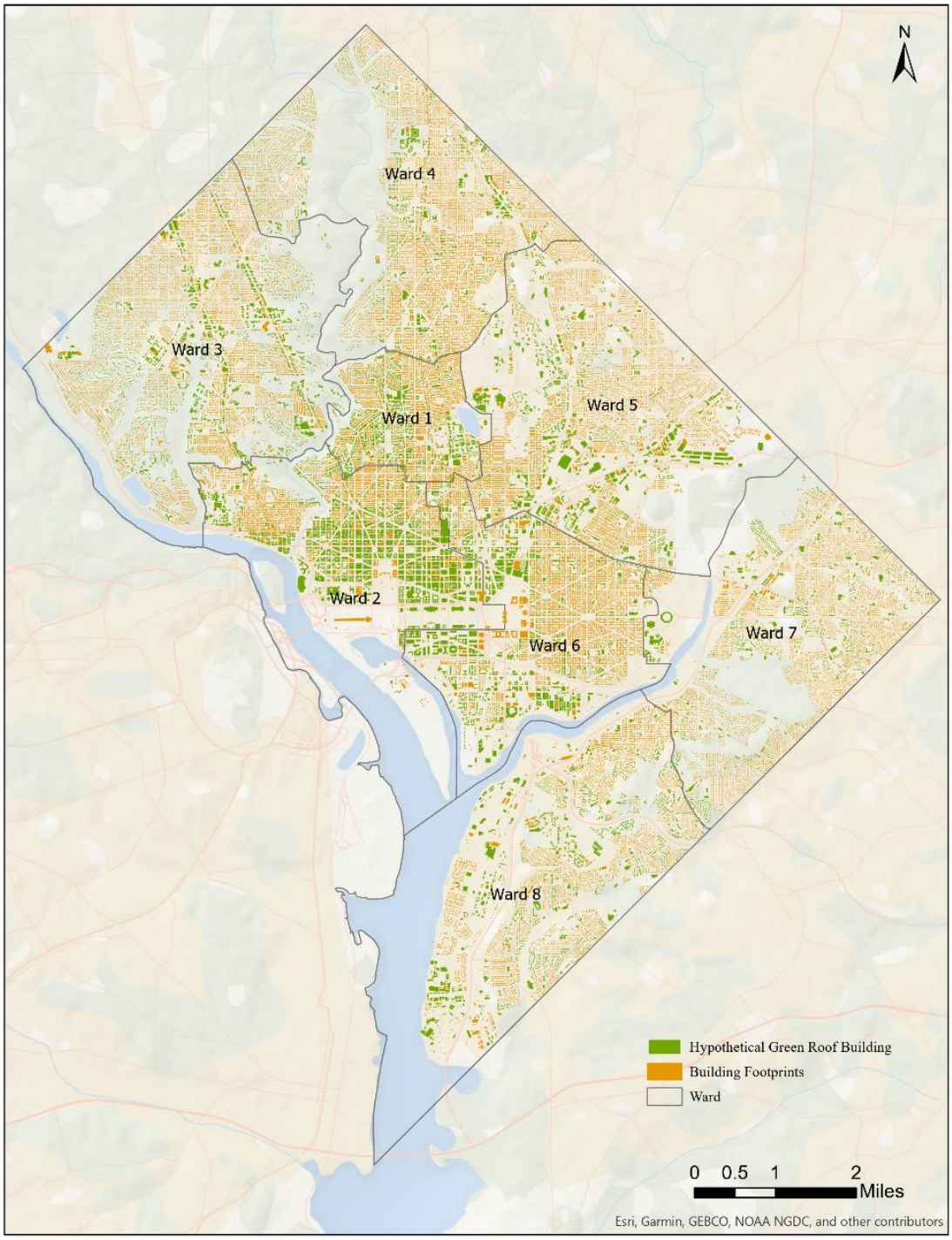

Figure 6. Distribution of selected buildings for scenario 1.

I compared the mean temperature of impervious surface areas before and after installing green roofs with the mean temperature of the pervious surface areas to find the

IUHI temperature. Results show that before hypothetical green roof installations an IUHI exists in the months examined—that the impervious (urban) temperature is greater than the pervious (rural) temperature by between 2.26 ℃ to 4.09 ℃ (Table 12). The IUHI lessens after hypothetical green roof installations by between 0.12 ℃ and 0.19 ℃. In January, where it previously did not show a significant temperature differences among conventional and green roofs, installing green roofs did not make significant temperature differences within the city (as expected). Even though there is no surface temperature differences in January between urban and rural, installing green roofs is still important since during winter, green roofs act as wind shields and reduce heating loads in buildings (Khan & Asif, 2017).

Table 12: Temperature of pervious and impervious areas before and after hypothetical green roof installation.

		May	July	August	September	October	January
pervious		26.71	31.92	31.79	26.19	19.00	4.30
impervious	before green roofs	28.97	36.01	35.39	28.57	21.10	4.40
	after green roofs	28.78	35.83	35.21	28.45	20.93	4.40
IUHI	before green roofs	2.26	4.09	3.6	2.38	2.1	0.1
	after green roofs	2.07	3.91	3.42	2.26	1.93	0.1
	differences	0.19	0.18	0.18	0.12	0.17	0

Table 13: 95% confidence interval on impervious surface temperature after hypothetical green roof installation for the first scenario.

Month			Upper and Lower Confidence values
May	Lower interval	28.67	0.11
	mean	28.78	
	Upper interval	28.88	0.10
July	Lower interval	35.72	0.11
	mean	35.83	
	Upper interval	35.93	0.10
Aug	Lower interval	35.11	0.10
	mean	35.21	
	Upper interval	35.31	0.10
Sep	Lower interval	28.34	0.11

	mean	28.45	
	Upper interval	28.55	0.10
Oct	Lower interval	20.83	0.10
	mean	20.93	
	Upper interval	21.03	0.10

The IUHI decreases when ~10% of the buildings have green roofs installed and the IUHI difference before and after green roof installation is 0.19 ˚C in May and the IUHI differences in other months are a little smaller (Table 12). According to table 13, I can say that the mean temperature of impervious surface decrease $\pm$ 0.1 ˚C after green roof installation. While this result does not appear to provide clear evidence that this green roof scenario would lead to a reduced IUHI, there are reasons why it should be considered further. It is necessary to mention that the satellite overpass time is in the morning (10:45 CST (March 14th-November 7th images); 9:45 CST (November 7th to March 14th images)) before the day has warmed up. I would expect that once the day warmed up, the IUHI would be more pronounced. Therefore, 0.19 ˚C in the morning may grow to a larger difference between 2 and 4pm.

For this analysis I selected an equal distribution of hypothetically installed green roofs, but it is likely that different distributions will have different impacts on the IUHI. As Alexandri and Jones' (2008) claim, if green walls and roofs apply to only one block, it can create a small area of mitigated temperature. On the other hand, if it applies to the whole city, they could reduce the urban temperature to a human-friendly level and reduce the amount of energy used for cooling buildings from 32% to 100%.

Of course, these small temperature differences must also be considered as possible given that widespread installation of green roofs is unlikely because of their costs. Since the price of installing and maintaining the green roof is higher than

conventional roofs, not all buildings can afford installing a green roof because the cost of green roofs is more than conventional and cooling roofs. Their cost depends on many different factors besides maintenance costs, including: the type of green roof, the depth of the medium, the vegetation types, the drainage system type, etc (EPA, 2008). Considering this fact, I can say that the number of selected buildings could be very less than 10% in the reality.

For the second hypothetical green roof scenario, 4104 buildings were selected based on the modified City of Toronto bylaw criteria (Figure 7). These buildings have the gross floor area of greater than 2000 m^2 and are higher than 3 floors. As it is shown in Figure 7, most of the selected buildings are located in the city center (near the Capitol) in the "Downtown" zone. These buildings areas are generally larger and are farther away from the large green areas. Table 14 shows the results of hypothetical green roof installations on the IUHI in different months. In addition, Table 15 provides the confidence intervals of hypothetical green roof installation for each month.

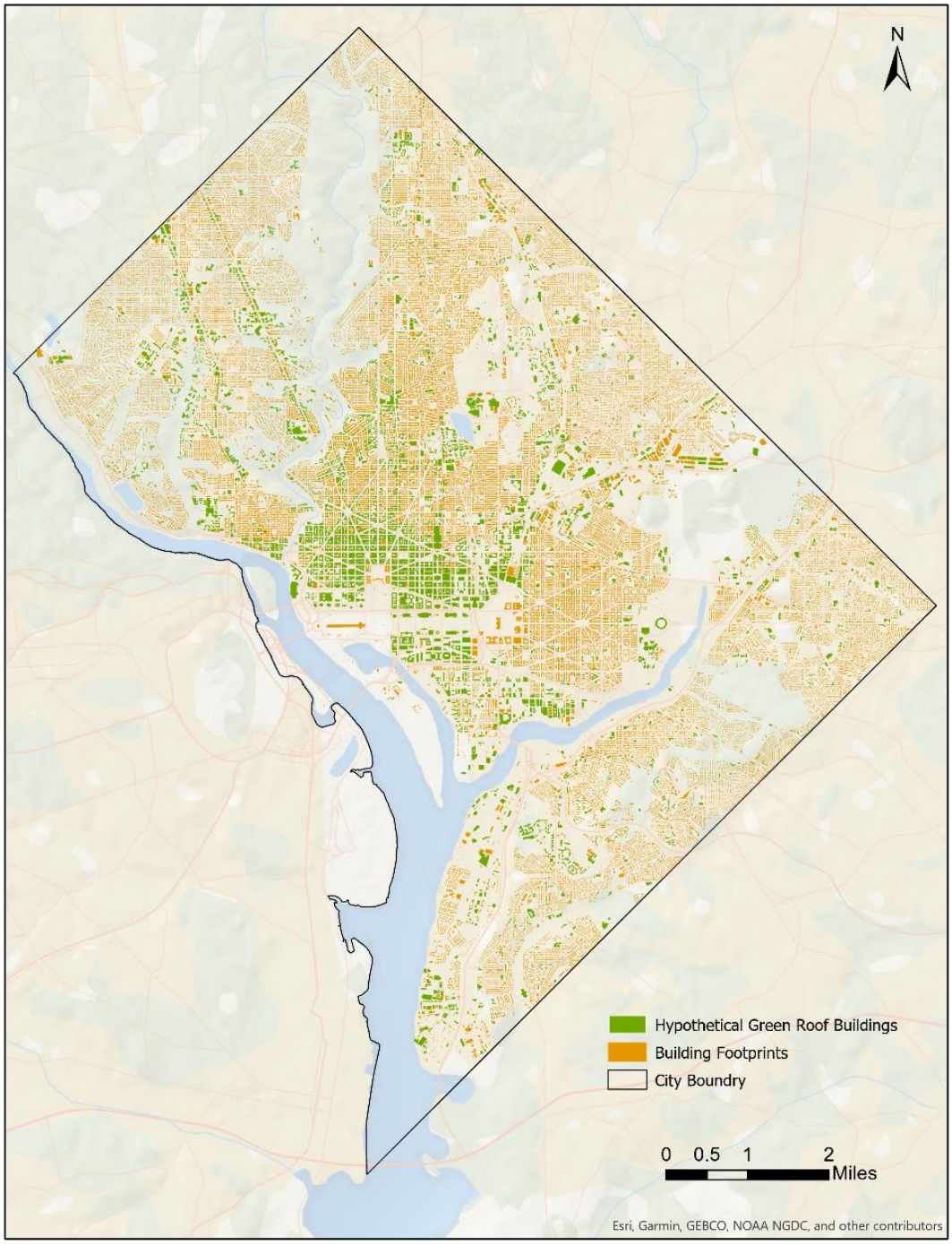

Figure 7. Distribution of selected buildings following the modified City of Toronto green roof bylaw.

Table 14: Temperature of pervious and impervious areas before and after hypothetical green roof installation.

		May	July	August	September	October	January
pervious		26.69	31.92	31.80	26.19	19.01	4.30

impervious	before green roofs	28.97	36.01	35.39	28.57	21.10	4.41
	after green roofs	28.88	35.93	35.31	28.51	21.03	4.37
IUHI	before green roofs	2.28	4.09	3.59	2.38	2.09	0.11
	after green roofs	2.19	4.01	3.51	2.32	2.02	0.07
	differences	0.09	0.08	0.08	0.06	0.07	0.04

Table 15: 95% confidence interval on impervious surface temperature after hypothetical green roof installation for the second scenario.

Month			Upper and Lower Confidence values
May	Lower interval	28.85	0.03
	mean	28.88	
	Upper interval	28.92	0.04
July	Lower interval	35.90	0.03
	mean	35.93	
	Upper interval	35.97	0.04
Aug	Lower interval	35.28	0.03
	mean	35.31	
	Upper interval	35.31	0.03
Sep	Lower interval	28.48	0.03
	mean	28.51	
	Upper interval	28.56	0.05
Oct	Lower interval	21.00	0.03
	mean	21.03	
	Upper interval	21.07	0.04

As Table 14 shows, by installing 4104 buildings, which account for only 0.26% of all buildings in the city, the IUHI temperature is slightly cooler than before installing green roofs. The IUHI differences are 0.09° C, 0.08° C, 0.08° C, 0.06° C, and 0.07° C in May, July, August, September and October, respectively. According to the table 15, the temperature of impervious surface could be $\pm$ 0.03 of the mean value in the same table. Therefore, the results show that green roof installation can make a difference in the microclimate temperature, as the consequence it reduces the IUHI temperature. It is essential to mention again that the temperatures are based on an image that collected data

at around 10am—too early for the IUHI to have fully developed during the day. These ~0.1 ˚C differences will likely grow larger and be more significant between 2 and 4pm.

Two spatial profiles for the month of July—the warmest month in 2019 — intersect in Figure 8. Cooler and hotter areas on the map correspond with the ups and downs in the figure. As expected, the lowest temperatures corresponded to the largest green areas in the city, Rock Creek Park and Piney Branch Parkway, in the northwest of the city (Figure 8, ellipse 1). In the contrast, the hottest spots in the city are located in the Production, Distribution, and Repair zone, in the central east of the city (Figure 8, ellipse 2 and 6). In this zone, heavy commercial and light manufacturing activities that require some heavy machinery are allowed. There is a cool area in southeast of the city (Fort circle park) which shows a drop in the spatial profile (Figure 8, ellipse 4). According to Figure 2, there is an approximately 20 ˚C difference in the coolest and hottest areas within Washington D.C. city border. There are two high peaks in Figure 8, ellipse 3, which corresponds to two river branches. Figure 8, ellipse 5 is the Potomac river and is constantly high over the river section. Water retains heat longer, therefore it shows higher temperature within the city. In fact, water maintains a relatively constant temperature compared to land. Often the water is warmer at night and the land is warmer in the day. That the water is so much warmer in the images is likely evidence that the land has not really warmed up yet because it is still morning (As mentioned before the satellite images have taken around 10 am). I would consider this as evidence that the IUHI that is evident in both scenarios is significant. I expect that the IUHI will become more pronounced later in the day. Observing that IUHI already exists in the morning is interesting. The fact that green roofs make a difference in the morning is more interesting and important. In an

ideal world we would have late afternoon thermal imagery so we could see the IUHI better.

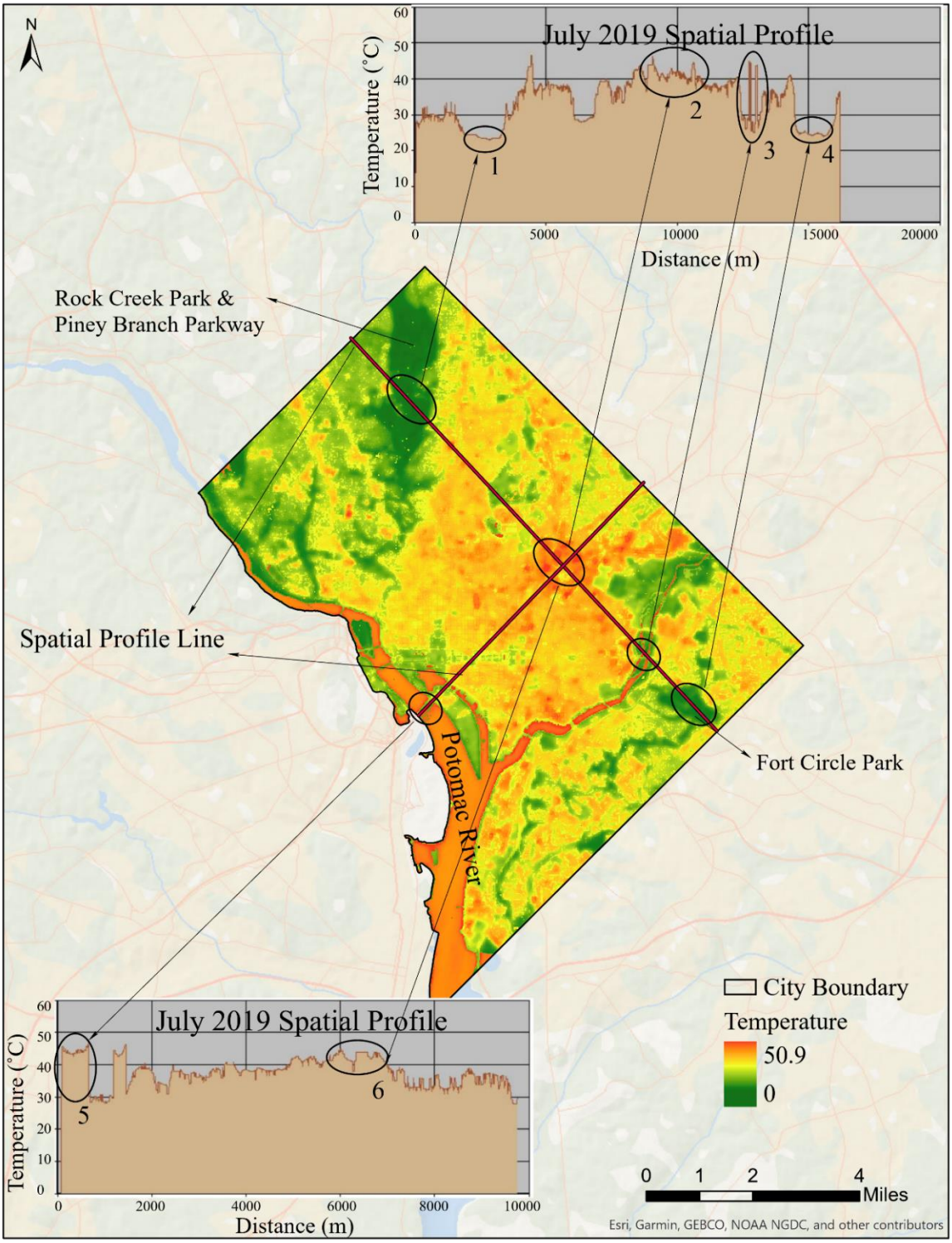

Figure 8. July 2019 spatial profile.

In both scenarios installing green roofs reduced rooftop temperatures and the IUHI. As mentioned aerlier, the configuration of green areas in a city can be as important as the size of the green areas in reducing the ambient temperature and it can influence the urban thermal characteristics (Asgarian, Amiri, & Sakieh, 2015; Chen & Yu, 2017). Selecting buildings with greater areas and in the downtown area where there is not much green spaces had a greater impact on mitigating the IUHI. The result of this research is aligned with the finding of other research like Santamouris (2014),who used controlled experiments that suggested very important climate benefits and a large reduction of the urban heat island by applying mitigation techniques.

5.4. Conclusion

For the first objective of this chapter, I hypothetically converted the rooftop temperature of 10% of the buildings in each of eight Wards in Washington D.C. to the green roofs' temperature by using Table 9 values for five warm months of the year (May, July, August, September, and October) and January as a cold month. By comparing the temperature of impervious surface before and after green roof installation, the results show a significant temperature differences between conventional and green roof after hypothetical green roof installation in the warm month of the year. Other than month of the year, we already know that the type of the green roof (extensive, intensive), the size of the green areas on the rooftop, the climate of the city, the type of plants on the roof, and many other factors can impact the effectiveness of green roofs in reducing the rooftop temperature. I believe that the result of this research, as the first study of this

kind, should give us a good start point to find more about the actual impact of green roofs in practice.

For the second objective of this chapter, I used a modify version of "Toronto Green Roof Bylaw" and selected 4104 Buildings. After converting the temperature of each one of them to a green roof temperature by using Table 9, I compared the temperature for impervious surface before and after green roof installation. The temperature of impervious surfaces is slightly cooler after converting the buildings' rooftop temperatures to green roof temperatures. This result again confirms that how installing green roof even on a small portion of impervious areas across city can contribute in colling down the rooftop surface temperature.

Based on Smart Cities Dive website (March 2021), the "North American green roof and wall industry association, Green Roofs for Healthy Cities (GRHC) has dubbed Washington D.C., the city with the greatest square footage of green roof installations in 2017. The District registered more than 1 million square feet of green roofs". Casey Trees, a nonprofit organization, proposed the 20-20-20 vision which propose 20 million ft^2 by 2020 (Niu, Clark, Zhou, & Adriaens, 2010). Although Washington D.C. is ranked one for green roof installation, the installed green roofs were slightly greater than 1 million square feet in 2017. "Despite the growth of the green roof industry, there is still an enormous potential for green roofs to be installed on billions of square feet of rooftops across North America. Policy support in cities like Washington, D.C. and Toronto is helping to drive market growth" (Living Architecture Monitor, July 2018). The result of this research clearly shows the importance of installing green roofs in Washington D.C., where apparently the process of installing green roofs is not going as fast as planned.

According to the U.S. Environmental Protection Agency (2008), the cost of different types of green roofs can be vary from $\$100/m^2$ to $\$250/m^2$ in United States. They mention that the installation price may decline when market demand and contractor experience increase. Over the lifetime of the green roof (40 years), the net present value is about 30-40% less than that of conventional roofs (not including green roof maintenance costs). These considerable benefits, in concert with current and emerging policy frameworks, may facilitate future adoption of this technology (Niu et al., 2010). Urban design can mitigate the urbanization impact where planners and policy makers increasingly notice that green roofs can be used to improve the urban environment quality (Williams et al., 2010). In this research, the positive effect of installing green roof in urban areas to mitigate urban heat indicates that this method can greatly reduce urban temperatures. With growing urban extents and increasing urban populations, green design and optimal spatial configuration of urban areas will matter for the reduction of urban heat.

In the existing literature, the mitigation potential of installing green roofs by applying the real-world data have not been extensively discussed, and only a few experiments (e.g. Dong et al., 2020) have been conducted to test the performance of green roof installation in mitigation UHI. My study filled this gap by estimating the mitigation performance of green roofs on hundreds of buildings across the Washington D.C. The main contribution of this study is that it examined the real cases of installed green roofs across a humid subtropical climate city, while considering the seasonal effect of installing green roofs. Moreover, results of the effectiveness of green roofs for decreasing rooftop temperatures were modeled using two hypothetical green roof

installation scenarios. These results provide valuable information to guide future policymaking. My approach has strong applicability due to the fact that all data are freely accessible on the opendata.dc.gov, so it can be used by other researchers in the future.

6. CONCLUSION

6.1. Summary

This chapter provides a summary of the major findings of this dissertation. It also discusses the main limitations of this study and finally makes recommendations for future studies. The main goal of this dissertation was to examine how green roof installations affected the SUHI in a dense city like Washington D.C. I designed three main objectives and the results are summarized as follows.

1) Detect the UHI in Washington D.C. by using processed satellite images and create the heat island map. Afterwards, perform conventional t-test to compare the temperatures of green and conventional roofed buildings.

I first created an urban heat map for the month of July using Landsat 8 satellite images. I used a set of criteria to select green roofs and conventional roofed buildings from among more than 161,000 buildings in Washington D.C. Of the 380 buildings identified in the official Washington, D.C. datasets as having green roofs, 156 were selected as actually having green roofs because they had an NDVI value greater than 0.25. By using the MatchIt package in R for propensity score matching, I selected 156 conventional roofs with similar attributes to the green roof buildings so I could compare their temperatures. A Welch two-sample t-test found that the green roof temperatures are significantly lower than conventional roof temperatures (the temperature differences was 1.1 ˚C). Therefore, the finding of this objective confirmed the benefit of installing green roofs in reducing IUHI in Washington D.C. Therefore, other dense cities with similar characteristics like similar climate, green spaces within the city, urban density could expect to benefit from installing green roofs.

2) Determine the month that the green roof has its highest impact on its ambient temperature by using 2-way ANOVA. Then, compare the rooftop temperatures before and after green roof installation by using post-treatment, difference-in-difference analysis and demonstrate the changing pattern of the urban temperature as a result of the green roofs installation.

In this section, I compared the rooftop temperatures of the 156 green roofs with their matched conventional roofs in each month of the year in 2019. The results shows that both month and treatment (i.e., the installation of a green roof) are significantly related to the rooftops' temperature. The Tukey pos-hoc test indicated that installing green roofs decreased the rooftop temperature. The temperature of green roofs is lower than conventional roofs by 1.08, 1.08, 1.05, 1.05 ˚C respectively in the months of May, July, August, and October, where the p-value is less than 0.05. Generally, we can see the pattern that green roof temperatures are cooler than conventional roofs in the warm months of the year in 2019, a finding that aligns with other studies.

In the contrast, comparing the rooftop temperatures of buildings before (2009) and after (2019) green roof installation using difference-in-difference regression did not show a significant difference. The results showed that treatment (installing a green roof) had a negative effect (it reduced the rooftop temperature) but this pattern was not statistically significant. This result was not aligned with my expectation, but it could be because I did not have enough samples to use for statistical tests. Among 156 green roof buildings in 2019, only eight of them had installed green roof before 2009. Besides the small sample size, the small size of the buildings, the relatively recent installations of

green roofs in 2009, and the relatively coarse resolution thermal images are possible explanations for the insignificant relationship.

3) Create a model of Washington D.C. by applying green roof temperatures to the selected building rooftops to see the result of the hypothetical installation of green roofs on those buildings in D.C.

I created two hypothetical scenarios of green roof installation in Washington D.C. For the first scenario I used specific criteria (explained in chapter 5) and selected 10% of the conventional roof buildings in each ward (approximately 12,000 buildings total) to hypothetically convert them to green roofs. The conversion to a green roof was accomplished by subtracting the amount that green roofs were found to be cooler than conventional roofs. The actual amount subtracted was drawn from by sampling the lower and upper 95% confidence interval for green roof temperature reductions. For the second scenario, buildings were selected solely based on the Toronto green roof bylaw criteria. This selection returned 4,104 conventional roof buildings which then were hypothetically converted to green roofs in the same way described above. The results of the first scenario showed that during warm months of the year the IUHI decreased. This finding links with the previous findings in chapter 3 and 4 where they confirmed that the green roofs were significantly cooler than conventional roofs in warm months of the year. The result of the second scenario showed a slightly larger reduction in the IUHI from the hypothetical installation of green roofs. Therefore, the results showed that green roof installation made a difference in the microclimate temperature and, as the consequence, the IUHI was reduced.

The urban heat island is not a new phenomenon; it has been more than a century since the term “urban heat island” was first introduced by scientists to describe how the urban temperature was undesirably higher than its surroundings rural areas. Climate change, human activity, urbanization, population growth, and other factors have accelerated this phenomenon. Therefore, it is important for governments, city managers and urban residents to find a practical approach to mitigate urban heat at low cost. While installing green roofs has been suggested as an effective method to cool rooftops and consequently mitigate the UHI, there has not been much research done about the actual implementation of green roofs in reducing surface temperatures across a city. Furthermore, the ability of green roofs to reduce rooftop temperatures in different seasons is another important element that needed to be evaluated when considering the effectiveness of green roofs in reducing rooftop temperatures. Among several studies on green roof implementations which were conducted using a small in-situ experiment, most focused on a single location without considering the context of the building (proximity to green areas, building height, building density, etc.) that affects the LST derived by satellite images. In this research I addressed these shortcomings in previous research by conducting my research on the spatial distribution of actual green roof installations in different seasons and years.

In the existing literature, there is much research about the benefits of installing green roofs for managing storm water runoff, and saving energy for building heating/cooling purposes (H. Akbari, 1992; Carter & Fowler, 2008; Elliott et al., 2016; Khan & Asif, 2017; Y. Li & Babcock, 2014, 2014; Susca et al., 2011). These studies were restricted to small study areas on single buildings or on a few selected buildings. In

addition, there are several studies about the role of green roofs in reducing rooftop temperatures by analyzing small samples of green roof installed on a building rooftop or by performing a mathematical model of green roof impact on building temperatures (Alexandri & Jones, 2008; Khan & Asif, 2017; J. K. W. Wong & Lau, 2013). On the other hand, remote sensing satellites have been used widely to provide land surface temperature continuously. There are only a few studies that analyze green roof temperatures and that draw conclusions about their effectiveness at reducing building temperatures and which ultimately result in UHI reduction (Dong et al., 2020). The mitigation potential of installing green roofs by applying real-world data have not been extensively discussed in previous research. My study filled this gap by estimating the mitigation performance of green roofs on hundreds of buildings across Washington D.C. by using satellite thermal images. The main contribution of this study is that it examined actual cases of installed green roofs across a humid subtropical climate area, while considering the seasonal effect of installing green roofs. The result of the first objective shows that buildings with green roof have lower temperature than other conventional roof buildings. While we can confirm the benefit of installing green roof in reducing LST, we run the second analysis steps to find out the month(s) of green roof effectiveness. While we know that the season is correlated to the strength of UHI (Santamoris, 2014), and during warm month of the year the UHI is more intense (Schatz 2014), it was important to determine the seasonal effectiveness of green roofs. The result of the second objective of this study confirmed that installing green roofs can positively impact rooftops to have cooler temperature during warm months of the year. While the cooling effect of installing green roofs has been frequently modeled (Razzaghmanesh; Alexandri and jones 2008;

Asadi 2020), my case study showed the overall temperature reduction in IUHI during warm month of the year over impervious surface areas. The results of hypothetical green roof installation and their benefits provide valuable information to guide future policymaking. These findings provide the empirical proof for the cooling effect of green roof on UHI in a dense city and important insights for urban planners and government agencies for the effective mitigation of UHI impacts.

6.2. Limitations and Recommendations

In recent years remote sensing satellites have been used widely to provide continuous land surface temperature (LST) measurements. Although the land surface temperature is not equal to the air temperature in the urban canopy layer, studies have confirmed that LST is highly correlated with near ground air temperature and is a reliable means of examining the relationship between UHI and urban surface parameters (Dong et al., 2020; Voogt & Oke, 2003). Certain limitations of the study arose because of the characteristics of the Landsat 8 imagery used in this study. The coarse resolution of Landsat 8 thermal images (30 m after resampling) and the effect this had on the calculation and aggregation of rooftop temperatures was one of the biggest limitations of this research. The thermal images were resampled from 100-meter resolution to the 30-meter resolution using cubic convolution resampling (which estimates the temperature of each pixel by using weighted average of 16 surrounding pixels) and this likely exacerbated the calculation and aggregation of rooftop temperatures. Since the study area is a dense city, the mixed pixel problem is likely to happen for the thermal satellite images. But until finer resolution images (from the potential HyspIRI mission, for

example) become available, we must deal with the resolution constraints of Landsat and ASTER thermal imagery. Also, the time of the day that the images were captured (11:46 a.m. EDT), where solar radiation might not have reached the ground in areas with high buildings, could result in a different temperature than the real one. In addition, the shade of neighboring buildings may cause underestimation of the surface temperature in the thermal images as well. These issues and shortcomings could be mediated with finer resolution thermal images if they become available in the future.

In this study, not enough data was collected on the details of buildings rooftops. Finding out the types of roof (e.g., cool roof or asphalt roof) and categorizing the city rooftop types can help to have more accurate inputs for comparing rooftop temperatures. One possible, indirect way to identify cool roofs (assuming they are white) would be to use satellite images with a finer spatial resolution (e.g., PlanetScope imagery with about a 4-meter spatial resolution). This could ensure that green roof temperatures are only compared to conventional roof temperatures instead of to other cool rooftops (Coutts et al., 2013). The type of green roofs, types of cultivated plants, and the amount of plants can greatly affect the green roof cooling effect (Khan & Asif, 2017; Wolf & Lundholm, 2008). It is recommended that for future studies, the details of green roofs be collected and be used in the analysis to find the relationship of green roof types and their effect on temperature.

REFERENCES

Agam, N., Kustas, W. P., Anderson, M. C., Li, F., & Neale, C. M. U. (2007). A vegetation index based technique for spatial sharpening of thermal imagery. *Remote Sensing of Environment*. https://doi.org/10.1016/j.rse.2006.10.006

Akbari, H. (1992). CoolingOur Communities A Guidebook On Tree Planting And Light-ColoredSurfacing. *City*. Retrieved from https://escholarship.org/uc/item/98z8p10x

Akbari, Hashem, Menon, S., & Rosenfeld, A. (2009). Global cooling: Increasing world-wide urban albedos to offset CO2. *Climatic Change*, *94*(3–4), 275–286. https://doi.org/10.1007/s10584-008-9515-9

Akbari, Hashem, & Rose, L. S. (2008). Urban Surfaces and Heat Island Mitigation Potentials. *Journal of the Human-Environment System*, *11*(2), 85–101. https://doi.org/10.1618/jhes.11.85

Alexandri, E., & Jones, P. (2008). Temperature decreases in an urban canyon due to green walls and green roofs in diverse climates. *Building and Environment*, *43*(4), 480–493. https://doi.org/10.1016/j.buildenv.2006.10.055

Asadi, A., Arefi, H., & Fathipoor, H. (2020). Simulation of green roofs and their potential mitigating effects on the urban heat island using an artificial neural network: A case study in Austin, Texas. *Advances in Space Research*, *66*(8), 1846–1862. https://doi.org/10.1016/j.asr.2020.06.039

Asgarian, A., Amiri, B. J., & Sakieh, Y. (2015). Assessing the effect of green cover spatial patterns on urban land surface temperature using landscape metrics approach. *Urban Ecosystems*. https://doi.org/10.1007/s11252-014-0387-7

Ashraf Muharam, ElSayed Amer, N. A.-H. (2016). IJAERS: Thermal Performance of the Extensive Green Roofs in Hot Dry Climate. *International Journal of Advanced Engineering Research and Science (IJAERS)*.

Azevedo, J., Chapman, L., & Muller, C. (2016). Quantifying the Daytime and Night-Time Urban Heat Island in Birmingham, UK: A Comparison of Satellite Derived Land Surface Temperature and High Resolution Air Temperature Observations. *Remote Sensing*, *8*(2), 153. https://doi.org/10.3390/rs8020153

Bai, X., McPhearson, T., Cleugh, H., Nagendra, H., Tong, X., Zhu, T., & Zhu, Y.-G. (2017). Linking Urbanization and the Environment: Conceptual and Empirical Advances. *Annual Review of Environment and Resources*, *42*(1), 215–240. https://doi.org/10.1146/annurev-environ-102016-061128

Banting, D., Doshi, H., Li, J., & Missious, P. (2005). Report on the environmental benefits and costs of green roof technology for the city of Toronto. In *OCE-ETech*.

Bengtsson, L., Grahn, L., & Olsson, J. (2004). Hydrological function of a thin extensive green roof in southern Sweden. *Nordic Hydrology*.

Berardi, U., GhaffarianHoseini, A., & GhaffarianHoseini, A. (2014). State-of-the-art analysis of the environmental benefits of green roofs. *Applied Energy*, *115*, 411–428. https://doi.org/10.1016/j.apenergy.2013.10.047

Blanusa, T., Vaz Monteiro, M. M., Fantozzi, F., Vysini, E., Li, Y., & Cameron, R. W. F. (2013). Alternatives to Sedum on green roofs: Can broad leaf perennial plants offer better "cooling service"? *Building and Environment*, *59*, 99–106. https://doi.org/10.1016/j.buildenv.2012.08.011

Bowler, D. E., Buyung-Ali, L., Knight, T. M., & Pullin, A. S. (2010). Urban greening to cool towns and cities: A systematic review of the empirical evidence. *Landscape and Urban Planning*. https://doi.org/10.1016/j.landurbplan.2010.05.006

Campra, P., Garcia, M., Canton, Y., & Palacios-Orueta, A. (2008). Surface temperature cooling trends and negative radiative forcing due to land use change toward greenhouse farming in southeastern Spain. *Journal of Geophysical Research Atmospheres*, *113*(18). https://doi.org/10.1029/2008JD009912

Carter, T., & Fowler, L. (2008). Establishing green roof infrastructure through environmental policy instruments. *Environmental Management*. https://doi.org/10.1007/s00267-008-9095-5

Chen, Y., & Yu, S. (2017). Impacts of urban landscape patterns on urban thermal variations in Guangzhou, China. *International Journal of Applied Earth Observation and Geoinformation*. https://doi.org/10.1016/j.jag.2016.09.007

Cheval, S., & Dumitrescu, A. (2015). The summer surface urban heat island of Bucharest (Romania) retrieved from MODIS images. *Theoretical and Applied Climatology*. https://doi.org/10.1007/s00704-014-1250-8

City of Toronto. (2012). Green Roof Bylaw. *Green Roofs*, 1–17.

Coseo, P., & Larsen, L. (2014). How factors of land use/land cover, building configuration, and adjacent heat sources and sinks explain Urban Heat Islands in Chicago. *Landscape and Urban Planning*. https://doi.org/10.1016/j.landurbplan.2014.02.019

Coutts, A. M., Daly, E., Beringer, J., & Tapper, N. J. (2013). Assessing practical measures to reduce urban heat: Green and cool roofs. *Building and Environment*, *70*, 266–276. https://doi.org/10.1016/j.buildenv.2013.08.021

Di Giuseppe, E., & D'Orazio, M. (2015). Assessment of the effectiveness of cool and green roofs for the mitigation of the Heat Island effect and for the improvement of thermal comfort in Nearly Zero Energy Building. *Architectural Science Review*, *58*(2), 134–143. https://doi.org/10.1080/00038628.2014.966050

Dong, J., Lin, M., Zuo, J., Lin, T., Liu, J., Sun, C., & Luo, J. (2020). Quantitative study on the cooling effect of green roofs in a high-density urban Area—A case study of Xiamen, China. *Journal of Cleaner Production*, *255*, 120152. https://doi.org/10.1016/j.jclepro.2020.120152

Durhman, A. K., Bradley Rowe, D., & Rugh, C. L. (2006). Effect of watering regimen on chlorophyll fluorescence and growth of selected green roof plant taxa. *HortScience*.

Elliott, R. M., Gibson, R. A., Carson, T. B., Marasco, D. E., Culligan, P. J., & McGillis, W. R. (2016). Green roof seasonal variation: Comparison of the hydrologic behavior of a thick and a thin extensive system in New York City. *Environmental Research Letters*. https://doi.org/10.1088/1748-9326/11/7/074020

Elmqvist, T., Bai, X., Frantzeskaki, N., Griffith, C., Maddox, D., McPhearson, T., … Watkins, M. (Eds.). (2018). *Urban Planet*. https://doi.org/10.1017/9781316647554

Elmqvist, T., Goodness, J., Marcotullio, P. J., Parnell, S., Sendstad, M., Wilkinson, C., … Seto, K. C. (2013). Urbanization, biodiversity and ecosystem services: Challenges and opportunities: A global assessment. In *Urbanization, Biodiversity and Ecosystem Services: Challenges and Opportunities: A Global Assessment*. https://doi.org/10.1007/978-94-007-7088-1

EPA: https://www.epa.gov/heat-islands

EPA, 2008. Reducing Urban Heat Islands: Compendium of Strategies (October 2008); Green Roofs. Available at: https://19january2017snapshot.epa.gov/sites/production/files/2014-06/documents/greenroofscompendium.pdf

Farrell, C., Szota, C., Williams, N. S. G., & Arndt, S. K. (2013). High water users can be drought tolerant: using physiological traits for green roof plant selection. *Plant and Soil*. https://doi.org/10.1007/s11104-013-1725-x

Getter, K. L., Rowe, D. B., & Andresen, J. A. (2007). Quantifying the effect of slope on extensive green roof stormwater retention. *Ecological Engineering*. https://doi.org/10.1016/j.ecoleng.2007.06.004

Gill, S. E., Handley, J. F., Ennos, a R., & Pauleit, S. (2007). Adapting cities for climate change: The role of the green infrastructure. *Built Environment*, *33*(1), 115–133. https://doi.org/10.2148/benv.33.1.115

Gregoire, B. G., & Clausen, J. C. (2011). Effect of a modular extensive green roof on stormwater runoff and water quality. *Ecological Engineering*. https://doi.org/10.1016/j.ecoleng.2011.02.004

Herman, R. (2003). Green roofs in Germany: yesterday, today and tomorrow. *Greening Rooftops for Sustainable Communities*.

Howard, Luke. 1818. The Climate of London: deduced from Meteorological observations, made at different places in the neighbourhood of the metropolis (W. Phillips, sold also by J. and A. Arch).

Huang, G., Zhou, W., & Cadenasso, M. L. (2010). Understanding the relationship between urban land surface temperature, landscape heterogeneity and social structure. *International Geoscience and Remote Sensing Symposium (IGARSS)*. https://doi.org/10.1109/IGARSS.2010.5649806

Kalantar, B., Mansor, S., Khuzaimah, Z., Sameen, M. I., & Pradhan, B. (2017). Modelling mean albedo of individual roofs in complex urban areas using satellite images and airborne laser scanning point clouds. *International Archives of the Photogrammetry, Remote Sensing and Spatial Information Sciences - ISPRS Archives*. https://doi.org/10.5194/isprs-archives-XLII-2-W7-237-2017

Khan, H., & Asif, M. (2017). Impact of Green Roof and Orientation on the Energy Performance of Buildings: A Case Study from Saudi Arabia. *Sustainability*, *9*(4), 640. https://doi.org/10.3390/su9040640

Kikon, N., Singh, P., Singh, S. K., & Vyas, A. (2016). Assessment of urban heat islands (UHI) of Noida City, India using multi-temporal satellite data. *Sustainable Cities and Society*. https://doi.org/10.1016/j.scs.2016.01.005

Kim, K. G. (2004). The application of the biosphere reserve concept to urban areas: The case of green rooftops for habitat network in Seoul. *Annals of the New York Academy of Sciences*, *1023*, 187–214. https://doi.org/10.1196/annals.1319.010

King, A. D., & Karoly, D. J. (2017). Climate extremes in Europe at 1.5 and 2 degrees of global warming. *Environmental Research Letters*. https://doi.org/10.1088/1748-9326/aa8e2c

Köhler, M. (2006). Long-term Vegetation Research on Two Extensive Green Roofs in Berlin. *Urban Habitats*.

Kyriakodis, G. E., & Santamouris, M. (2017). Using reflective pavements to mitigate urban heat island in warm climates - Results from a large scale urban mitigation project. *Urban Climate*. https://doi.org/10.1016/j.uclim.2017.02.002

Li, W. C., & Yeung, K. K. A. (2014). A comprehensive study of green roof performance from environmental perspective. *International Journal of Sustainable Built Environment*, *3*(1), 127–134. https://doi.org/10.1016/j.ijsbe.2014.05.001

Li, Y., & Babcock, R. W. (2014). Green roof hydrologic performance and modeling: A review. *Water Science and Technology*. https://doi.org/10.2166/wst.2013.770

MacIvor, J. S., & Lundholm, J. (2011). Performance evaluation of native plants suited to extensive green roof conditions in a maritime climate. *Ecological Engineering*. https://doi.org/10.1016/j.ecoleng.2010.10.004

McKinney, M. L. (2002). Urbanization, Biodiversity, and ConservationThe impacts of urbanization on native species are poorly studied, but educating a highly urbanized human population about these impacts can greatly improve species conservation in all ecosystems. *BioScience*, *52*(10), 883–890. Retrieved from http://dx.doi.org/10.1641/0006-3568(2002)052[0883:UBAC]2.0.CO

Metselaar, K. (2012). Water retention and evapotranspiration of green roofs and possible natural vegetation types. *Resources, Conservation and Recycling*. https://doi.org/10.1016/j.resconrec.2011.12.009

Mirzaei, P. A., & Haghighat, F. (2010). Approaches to study Urban Heat Island - Abilities and limitations. *Building and Environment*. https://doi.org/10.1016/j.buildenv.2010.04.001

Mohajerani, A., Bakaric, J., & Jeffrey-Bailey, T. (2017). The urban heat island effect, its causes, and mitigation, with reference to the thermal properties of asphalt concrete. *Journal of Environmental Management*. https://doi.org/10.1016/j.jenvman.2017.03.095

NASA. 2011. *Landsat 7 Science Data Users Handbook. National Aeronautics and Space Administration*. https://doi.org/10.1111/j.1547-5069.2012.01449.x.

National Weather Service- Washington D.C. temperature. https://www.weather.gov/media/lwx/climate/dcatemps.pdf

National Weather Service- Washington D.C. precipitation. https://www.weather.gov/media/lwx/climate/dcaprecip.pdf

Niu, H., Clark, C., Zhou, J., & Adriaens, P. (2010). Scaling of economic benefits from green roof implementation in Washington, DC. *Environmental Science and Technology*, *44*(11), 4302–4308. https://doi.org/10.1021/es902456x

NNJoin 3.1.3 documentation. http://arken.nmbu.no/~havatv/gis/qgisplugins/NNJoin/#

Oberndorfer, E., Lundholm, J., Bass, B., Coffman, R. R., Doshi, H., Dunnett, N., … Rowe, B. (2007). Green Roofs as Urban Ecosystems: Ecological Structures, Functions, and Services. *BioScience*. https://doi.org/10.1641/B571005

Oke, T. R. (1982). The energetic basis of the urban heat island (Symons Memorial Lecture, 20 May 1980). *Quarterly Journal, Royal Meteorological Society*, *108*(455), 1–24. https://doi.org/10.1002/qj.49710845502

Park, J.-H., & Cho, G.-H. (2016). Examining the Association between Physical Characteristics of Green Space and Land Surface Temperature: A Case Study of Ulsan, Korea. *Sustainability*, *8*(8). https://doi.org/10.3390/su8080777

Peng, J., Xie, P., Liu, Y., & Ma, J. (2016). Urban thermal environment dynamics and associated landscape pattern factors: A case study in the Beijing metropolitan region. *Remote Sensing of Environment*. https://doi.org/10.1016/j.rse.2015.11.027

Planet Labs. (2019). Planet Imagery Product Specification. *Planet Labs Inc*, (October), 56. Retrieved from https://www.planet.com/products/satellite-imagery/files/Planet_Imagery_Product_Specs.pdf

Razzaghmanesh, M., Beecham, S., & Salemi, T. (2016). The role of green roofs in mitigating Urban Heat Island effects in the metropolitan area of Adelaide, South Australia. *Urban Forestry and Urban Greening*, *15*, 89–102. https://doi.org/10.1016/j.ufug.2015.11.013

Roman, K. K., O'Brien, T., Alvey, J. B., & Woo, O. J. (2016). Simulating the effects of cool roof and PCM (phase change materials) based roof to mitigate UHI (urban heat island) in prominent US cities. *Energy*, *96*, 103–117. https://doi.org/10.1016/j.energy.2015.11.082

Santamouris, M. (2014). Cooling the cities - A review of reflective and green roof mitigation technologies to fight heat island and improve comfort in urban environments. *Solar Energy*, *103*, 682–703. https://doi.org/10.1016/j.solener.2012.07.003

Schatz, J., & Kucharik, C. J. (2014). Seasonality of the urban heat island effect in Madison, Wisconsin. *Journal of Applied Meteorology and Climatology*, *53*(10), 2371–2386. https://doi.org/10.1175/JAMC-D-14-0107.1

Seto, K. C., Sánchez-Rodríguez, R., & Fragkias, M. (2010). The New Geography of Contemporary Urbanization and the Environment. *Ssrn*. https://doi.org/10.1146/annurev-environ-100809-125336

Shen, H., Huang, L., Zhang, L., Wu, P., & Zeng, C. (2016). Long-term and fine-scale satellite monitoring of the urban heat island effect by the fusion of multi-temporal and multi-sensor remote sensed data: A 26-year case study of the city of Wuhan in China. *Remote Sensing of Environment*, *172*, 109–125. https://doi.org/10.1016/j.rse.2015.11.005

Simmons, M. T., Gardiner, B., Windhager, S., & Tinsley, J. (2008). Green roofs are not created equal: The hydrologic and thermal performance of six different extensive green roofs and reflective and non-reflective roofs in a sub-tropical climate. *Urban Ecosystems*. https://doi.org/10.1007/s11252-008-0069-4

Snodgrass, E. C., & Snodgrass, L. L. (2006). Green Roof Plants: A Resource and Planting Guide. In *Landscape Architecture*.

Stone, B., & Rodgers, M. O. (2001). Urban form and thermal efficiency. *Journal of the American Planning Association*. https://doi.org/10.1080/01944360108976228

Stovin, V., Poë, S., & Berretta, C. (2013). A modelling study of long term green roof retention performance. *Journal of Environmental Management*. https://doi.org/10.1016/j.jenvman.2013.09.026

Susca, T., Gaffin, S. R., Dell'osso, G. R., & Dell'Osso, G. R. (2011). Positive effects of vegetation: urban heat island and green roofs. *Environmental Pollution*, *159*(8–9), 2119–2126. https://doi.org/http://dx.doi.org/10.1016/j.envpol.2011.03.007

Team, H. M. C. (2018). HyspIRI Final Report. *HyspIRI Final Report*, (September), 91. Retrieved from https://hyspiri.jpl.nasa.gov/downloads/reports_whitepapers/HyspIRI_FINAL_Report_1October2018_20181005a.pdf

United Nations. (2014). World Urbanization Prospects 2014. In *Demographic Research*. https://doi.org/(ST/ESA/SER.A/366)

VanWoert, N. D., Rowe, D. B., Andresen, J. A., Rugh, C. L., & Xiao, L. (2005). Watering regime and green roof substrate design affect Sedum plant growth. *HortScience*. https://doi.org/10.2134/jeq2004.0364

Villarreal, E. L., & Bengtsson, L. (2005). Response of a Sedum green-roof to individual rain events. *Ecological Engineering*. https://doi.org/10.1016/j.ecoleng.2004.11.008

Voogt, J. A., & Oke, T. R. (2003). Thermal remote sensing of urban climates. *Remote Sensing of Environment*, *86*(3), 370–384. https://doi.org/10.1016/S0034-4257(03)00079-8

Walsh, C. J., Roy, A. H., Feminella, J. W., Cottingham, P. D., Groffman, P. M., & Morgan, R. P. (2005). The urban stream syndrome: current knowledge and the search for a cure. *Journal of the North American Benthological Society*.

Weng, Q. (2009). Thermal infrared remote sensing for urban climate and environmental studies: Methods, applications, and trends. *ISPRS Journal of Photogrammetry and Remote Sensing*, *64*(4), 335–344. https://doi.org/10.1016/j.isprsjprs.2009.03.007

Weng, Q., Lu, D., & Schubring, J. (2004). Estimation of land surface temperature-vegetation abundance relationship for urban heat island studies. *Remote Sensing of Environment*, *89*(4), 467–483. https://doi.org/10.1016/j.rse.2003.11.005

Weng, Q., Rajasekar, U., & Hu, X. (2011). Modeling urban heat islands and their relationship with impervious surface and vegetation abundance by using ASTER images. *IEEE Transactions on Geoscience and Remote Sensing*, *49*(10 PART 2), 4080–4089. https://doi.org/10.1109/TGRS.2011.2128874

Williams, N. S. G., Rayner, J. P., & Raynor, K. J. (2010). Green roofs for a wide brown land: Opportunities and barriers for rooftop greening in Australia. *Urban Forestry and Urban Greening*. https://doi.org/10.1016/j.ufug.2010.01.005

Wolf, D., & Lundholm, J. T. (2008). Water uptake in green roof microcosms: Effects of plant species and water availability. *Ecological Engineering*, *33*(2), 179–186. https://doi.org/10.1016/j.ecoleng.2008.02.008

Wong, J. K. W., & Lau, L. S. K. (2013). From the "urban heat island" to the "green island"? A preliminary investigation into the potential of retrofitting green roofs in Mongkok district of Hong Kong. *Habitat International*. https://doi.org/10.1016/j.habitatint.2012.10.005

Wong, N. H., Cheong, D. K. W., Yan, H., Soh, J., Ong, C. L., & Sia, A. (2003). The effects of rooftop garden on energy consumption of a commercial building in Singapore. *Energy and Buildings*. https://doi.org/10.1016/S0378-7788(02)00108-1

Yang, J., Yu, Q., & Gong, P. (2008). Quantifying air pollution removal by green roofs in Chicago. *Atmospheric Environment*, *42*(31), 7266–7273. https://doi.org/10.1016/j.atmosenv.2008.07.003

Yokobori, T., & Ohta, S. (2009). Effect of land cover on air temperatures involved in the development of an intra-urban heat island. *Climate Research*. https://doi.org/10.3354/cr00800

Zhang, Z., Szota, C., Fletcher, T. D., Williams, N. S. G., Werdin, J., & Farrell, C. (2018). Influence of plant composition and water use strategies on green roof stormwater retention. *Science of the Total Environment*, *625*, 775–781. https://doi.org/10.1016/j.scitotenv.2017.12.231

Zhao, C. (2018). Linking the local climate zones and land surface temperature to investigate the surface urban heat island, a case study of San Antonio, Texas, U.S. *ISPRS Annals of the Photogrammetry, Remote Sensing and Spatial Information Sciences*. https://doi.org/10.5194/isprs-annals-IV-3-277-2018